Modeling the Impacts of the Loop Current on Circulation and Water Properties over the Pulley Ridge Region on the Southwest Florida Shelf

Chudong Pan[*], Mingshun Jiang, Fraser Dalgleish, and John Reed

Abstract

A high-resolution (~1.5 km) regional ocean model was developed for the southern Florida Shelf and Florida Straits. A two-year (2011-12) simulation was conducted and the model results were generally in good agreement with available satellite and *in situ* data. Model results show that the meandering of the Gulf of Mexico Loop Current (LC) exerts strong impacts on the dynamics over Pulley Ridge on the southwest Florida shelf, where the LC turns into the Florida Straits to become the Florida Current (FC). In particular, the northward migration of the LC/FC front often drives strong on-shelf (eastward) transport of the slope water onto the shelf of southern Pulley Ridge, an important mesophotic coral reef at depths between 60 and 90 m. Frequent remotely or locally generated eddies over the western slope of Pulley Ridge may be blocked by the northern LC/FC front when it is closely in contact with the shelf break, a phenomenon documented in previous studies. These eddies drive strong upwelling of slope water toward the shelf break, which sometimes can extend 20-30km onto the shelf, strongly affecting the Pulley Ridge region. A narrow return flow, largely along the shelf edge from Florida Keys to Pulley Ridge, may be produced when the FC impinges upon the continental slope during late fall to early spring. The results from an experiment without the surface winds suggest that wind forcing contributes to the westward flow but is not the determining factor for its generation.

Keywords: **Gulf of Mexico, Pulley Ridge, Loop Current, Florida Current, meso-scale eddy, upwelling, cross-shelf transport**

1. Introduction

Pulley Ridge is a carbonate ridge that extends north-south at depths of 60-90 m for nearly 300 km along the southwestern Florida platform in the northern Gulf of Mexico and lies about 250 km west of the Florida coastline (Fig. 1; Hine et al., 2008). Southern Pulley Ridge is the southern terminus of this geological feature which supports a mesophotic coral ecosystem (MCE) at depths of 60-90 m (Cross et al., 2005; Reed, 2016). It has been described as the deepest, light-dependent coral reef on the U.S. continental shelf (Halley et al. 2004; Culter et al., 2006). Southern Pulley Ridge has been designated as Pulley Ridge Habitat Area of Particular Concern (PR HAPC, Fig. 1), which is a 346 km^2 marine reserve that is considered essential habitat for both coral and fish. Another coral reef habitat, Tortugas Ecological Reserve (TER, Fig. 1), located about 50 km east of PR HAPC, also breeds rare corals and fishes. Such productive benthic communities are sustained by several key environmental factors, including local dynamics, light availability, nutrients, water clarity and temperature, all of which are likely strongly impacted by the impingement of the Loop Current on the shelf margin (Jarrett et al., 2005).

The circulation on the West Florida Shelf (WFS) is mainly driven by local freshwater runoff, meteorological forcing, and the deep-ocean momentum and buoyancy fluxes transmitted across the shelf break (Weisberg and He, 2003; Weisberg et al., 2005). The circulation on the inner shelf is mainly driven by surface winds with additional nearshore freshwater plume due to local run-off, particularly during wet seasons (Weisberg et al., 1996; Weisberg et al., 2005; Liu and Weisberg, 2012). The circulation on the outer shelf, by contrast, is strongly affected by the Gulf of Mexico Loop Current (LC), a western boundary current that may interact with the shelf (e.g., Huh et al., 1981; Hetland et al., 1999; He and Weisberg, 2003a, b; Weisberg and He, 2003;

Weisberg et al., 2005; Weisberg et al. 2014a-c). The LC enters the Gulf of Mexico through the Yucatan Channel, and typically overshoots to the northern Gulf and then turns clockwise along the western Florida shelf slope, forming a wide loop in the eastern Gulf before it enters the Florida Straits to become the Florida Current (FC). Further downstream, the FC in turn becomes the origin of the Gulf Stream off the southeastern U.S. Depending on the extent of the intrusion into the Gulf, the LC interacts with the Gulf waters in different ways. For example, the LC could overshoot to the south of the Mississippi River Delta and entrain freshwater from the Mississippi river into the open ocean, which can subsequently be transported to the Dry Tortugas or even through the Florida Straits (e.g., Gilbert et al., 1996; Hu et al., 2005; Le Henaff et al., 2016). Much of the waters in the deep basin are transported from Caribbean to the Gulf of Mexico by the Loop Current (Rivas et al., 2005). The waters between 50 and 600m, are mainly from tropics and central north Atlantic but also from Sargasso Sea with a temperature range of 8-23^{o}C and salinity range of 35-35.7 psu (Rivas et al., 2005). Sometimes, the Loop Current turns directly into the Florida Straits without much overture into the Gulf. Over the southern slope near Dry Tortugas, a prominent near stationary meso-scale eddy may be formed due to the meandering and instability of the FC (e.g., Lee et al. 1994; Fratantoni et al., 1998; Lee and Williams, 1999). A countercurrent, ~ 5 cm sec^{-1} on annual average, may be present over the southern slope of the Dry Tortugas (e.g., Lee and Williams, 1999; Lee et al., 2001; Kourafalou et al., 2006).

A number of studies have been carried out to understand the interactions between the LC and the WFS waters (e.g., Hetland et al., 1999; He and Weisberg, 2003a, b; Weisberg and He, 2003; Weisberg et al., 2014a). Hetland et al. (1999) proposed that the pressure gradient between the deep ocean and the shelf set up by the LC near Dry Tortugas drives a narrow southward jet along the western shelf edge. Subsequent studies indicated that this pressure gradient may set the entire shelf water in motion and drive an on-shore intrusion (He and Weisberg, 2003a, b; Weisberg and He, 2003; Weisberg et al., 2005). This intrusion can potentially affect the water properties of the entire WFS, mainly through the onshore bottom Ekman transport when the shelf-edge jet moves toward the south (Weisberg et al., 2014a). The cold upwelled water associated with the jet from the northern WFS can even make its way to as far south as Dry Tortugas (Weisberg et al., 2014a).

Direct cross-shelf transport can also occur at certain segments of the shelf, but such events are rare. Using satellite and *in situ* observations, Huh et al. (1981) reported a LC intrusion event at De Soto Canyon off the northwest Florida shelf as the LC penetrated deeply into the northern Gulf. He and Weisberg (2003a) also investigated a LC intrusion case at the shelf break at the Tampa Bay and Sarasota segment using satellite data and the Princeton Ocean Model (POM).

This manuscript examines the potential local interactions between the LC and the shelf/slope over the Pulley Ridge region because of recent strong interest in the biogeochemical and ecological processes on these fragile mesophotic coral reefs. In this area, the shallow and deep isobaths converge and the shelf break (about 80 m isobath) makes a 90^{o} turn from north-south to almost west-east (Fig. 1). This is also the transition zone where the LC turns into the Florida Straits to become the FC. As a result, this is one of the most dynamic regions on the WFS (Weisberg et al., 2005). Most previous studies on the interactions between the LC and the shelf water mainly focused on the broad shelf break from Mississippi to Pulley Ridge. Recently, Kourafalou and Kang (2012) examined in details the evolution of cyclonic eddies in the Florida Keys and eddy propagation from western Florida shelf slope toward the Florida Straits. Yet it remains unclear how exactly the LC/FC and associated eddies may impact the Pulley Ridge region and how the unique geometrical features may affect the interactions between the LC/FC and the shelf/slope. To address these questions, a three-dimensional, high-resolution numerical model was developed for the southwest Florida shelf and Florida Straits. The model results were validated by comparing with autonomous underwater glider observations, satellite images, and other *in situ* data. In this manuscript, we specifically examine the impacts of the LC/FC on the meso-scale dynamics and water properties near Pulley Ridge by analyzing cross-shelf transport, eddy activities and associated upwelling events, and their relationships with the LC/FC.

The paper is organized as follows. The numerical model and the available observations are described in Section 2. In section 3, we present and verify the model results by comparing them with observations. In section 4, we present an analysis of the model results, and discuss the underlying physical phenomena and associated processes relevant to the Pulley Ridge region. Conclusions and summary are provided in section 5.

2. Numerical model and data

2.1. Numerical model

The numerical model is based on the Regional Ocean Modeling System (ROMS), which is a three-dimensional, prognostic, primitive equation ocean model with a vertical terrain-following sigma coordinate system (Shchepetkin and McWilliams, 2005). The model domain covers the southern Florida shelf, the Florida Straits, the northern part of the Cuba Island and the western part of the Great Bahamas Bank (Fig. 1). Horizontally, a uniform grid is used with a resolution of ~1.5 km. Vertically, the model has 35 sigma layers that are concentrated at the top layers. The numerical schemes for the model include the third-order upstream scheme for horizontal advection, fourth-order centered difference scheme for vertical advection in both the momentum and tracer equations, and the Generic Length Scale (GLS) closure (Umlauf and Burchard, 2003) for vertical turbulent mixing. A uniform horizontal viscosity of 5 m^2 sec^{-1} for currents and a uniform mixing coefficient of 5 m^2 sec^{-1} for tracers have been applied on the geopotential surfaces (Haidvogel and Beckmann, 1999). The model is driven by surface meteorological forcing, open boundary forcing, and the local run-offs (detailed below). Tidal forcing is not included.

The initial model state, including temperature, salinity, velocities and sea surface height, is extracted from the 1/25^o Gulf of Mexico (GOMex) Hybrid Coordinate Ocean Model (HYCOM, Chassignet et al., 2009, http://tds.hycom.org/thredds/catalog.html) output and linearly interpolated into the model domain. At the surface, the model is driven by the 3-hourly North American Regional Reanalysis (NARR, Mesinger et al., 2006, http://nomads.ncdc.noaa.gov/thredds/catalog/narr-a/) meteorological forcing, including wind stresses, longwave and shortwave (solar) radiations, latent and sensible heat fluxes, evaporation and precipitation. All the forcing variables have been linearly interpolated from the NARR grid into the model grid. In order to reduce sea surface temperature (SST) error, we relaxed the model SST to the observed daily SST from the Physical Oceanography Distributed Active Archive Center (PO. DAAC, http://podaac-opendap.jpl.nasa.gov/opendap/hyrax/allData/ghrsst/data/L4/). The model has three open boundaries (north, west and east) and a closed southern boundary (Fig. 1). Lateral boundary forcing is derived from the GOMex HYCOM (Prasad and Hogan, 2007). Along the boundaries, a radiation-nudging scheme has been applied to all model variables with a sponge layer of increased diffusion and viscosity within a buffer zone (20 grid points) in order to reduce boundary singularity. The modeling period is chosen as 2011-2012, but the simulation is repeated for several cycles to allow the model fields fully adjusting to the boundary forcing.

Local freshwater run-offs are an important part of the dynamical system, especially over the inner shelf of the WFS (Weisberg et al., 2005). There are a number of small to medium rivers in the western Florida coast, such as Caloosahatchee River, Peace River, Manatee River and Shark River. Currently, the model includes all the major rivers (total 32) with daily discharges derived from the U. S. Geological Survey (USGS) gauge data (http://waterdata.usgs.gov/nwis). If a river station is close to the river mouth, the river discharge might contain negative values (when flow is into the river) that are not compatible with ROMS. Therefore we extracted river discharge data from upstream stations and adjust the river flows based on the actual drainage area.

2.2. Data

In order to evaluate the model performance, we compared model results with observations collected from various sources, including underwater glider profiles, traditional CTD casts and satellite images. Detailed descriptions of available data used here are provided below.

Over the last decade, underwater gliders have been widely used for collecting high resolution data from surface down to the seafloor with high efficiency (e.g., Davis et al., 2002; Rudnick et al., 2004; Schofield et al., 2010). In September 11-November 10, 2011, a research cruise on the NOAA ship *Nancy Foster* (hereafter cruise I) was conducted in the Pulley Ridge region to survey the shelf-edge coral reef ecosystem using a Bluefin Spray glider, Remotely Operated Vehicle (ROV), as well as traditional CTD casts (Reed et al., 2012a, b). The glider was outfitted with a CTD, an elastic scattering sensor and a fluorescence sensor to collect temperature, salinity, turbidity and chlorophyll-a profiles respectively. The ship survey ended on September 30, 2011, but the glider remained in the water collecting data until November 10, 2011. A second cruise, aiming at Florida shelf edge exploration, organized by Cooperative Institute for Ocean Exploration, Research & Technology (CIOERT), took place in February 3-24, 2012 (hereafter cruise II), in which only the Spray glider with similar setup was used. Over 3200 dives were completed during cruise I and over 1000 dives were completed during the cruise II. The glider tracks are presented in both Fig. 1 (blue and red tracks) and Fig. 2 (focusing on Pulley Ridge). In cruise I, in addition to glider observations, vertical profiles of temperature and salinity were also collected using standard CTD casts at 19 stations (orange diamonds, Fig. 1) during the ship survey period. The stations can be separated into two groups: stations 01-13 were concentrated over southern Pulley Ridge region, close to the initial locations of the glider, while stations 14-19 were over the Pourtalès Terrace in the southern Florida Straits.

Two Gulf of Mexico and East Coast Carbon Cruises (GOMECC and GOMECC2) were conducted in 2007 and 2012, respectively, to measure hydrological and carbonate chemistry parameters in the Gulf of Mexico and along the east coast of U.S. (Wang et al., 2013; Wanninkhof et al., 2015). Here we use data from bottled samples during the second cruise, which covered the period of July 22 – August 13, 2012. Two transects of the cruise with a total of 19 stations are located within our model domain (Fig. 1).

As part of the a integrated global observation platform, the Argo Float program (http://www.argo.ucsd.edu/) utilizes free-drifting profiling floats to measure temperature and salinity down to 2000 m deep (e.g., Davis et al., 1992). During August 27 to December 13, an Argo float entered the Florida Straits from Gulf of Mexico, providing a total of 24 profiles of temperature and salinity in the Florida Straits (Fig. 1). These Argo data are used to verify the model results.

Remote sensing data are important because of their good spatial-temporal coverage. Here we compare model results with the daily sea surface height (SSH) from the Archiving, Validation and Interpretation of the Satellite Oceanographic (AVISO, http://www.aviso.altimetry.fr/) near real-time product with a resolution of 0.25^{o}.

From 1984 to 2003, in-situ observations were made at a series of stations with variable durations in Florida Bay and Florida Reef Tract (FRT) along the Florida Key islands, with the purpose of studying the circulation and water exchange between the Florida Bay and surrounding areas (Lee et al., 2002). The measured parameters include currents, temperature, conductivity, salinity, pressure, water levels and density, but only a subset of these parameters was measured at some stations. One of these stations was located on the southern edge of the FRT at a water depth of 32m. The data collected at this site is used in this study to compare with the modeled currents.

3. Model – data comparison

3.1. Glider profiles

A comparison between the Bluefin Spray glider observations and ROMS results is presented in Figs. 3 and 4. Model output was extracted at the grid points and times that were closest to the glider locations and surface times. During cruise I, the Spray glider was deployed near southern Pulley Ridge in early fall of 2011, when the water column was still strongly stratified. The glider was initially piloted northward along the shelf edge, then directed northeastward across the shelf around October 15. A few days later, it was piloted back toward the shelf edge, and after crossing the 70m isobath, it moved southward along the shelf edge before returning toward the north on around October 23. This time the glider was entrained into a meso-scale eddy circling the shelf edge for 5-6 days until the end of October, when it successfully moved northeastward about 60 km into the mid-shelf.

Both temperature and salinity profiles recorded along the glider path showed a slow trend of deepening thermocline and halocline, but the halocline trend was more pronounced (Fig. 3a, c).

By the end of glider survey, when the glider was in the mid-shelf (Fig. 2), the entire water column was well mixed (Fig. 3). A strong mixing event was observed during October 16-19, 2011, when both temperature and salinity values showed little vertical variation. Over this period, the wind direction took a sharp turn from southeasterly to northwesterly, with wind speed of approximately 14 m s^{-1}, according to the wind records from National Data Buoy Center (NDBC) station 42003 (26.00^{o}N, 85.65^{o}W).

Overall, the model was able to reproduce the general vertical structure of the water column along the glider path, including the deepening of the thermocline and halocline, and the strong mixing event, although modeled vertical mixing appeared to be weaker during the event (Fig. 3b, d). Modeled depth of the halocline was relatively deeper than the observed, especially during the first half of the track (September 26-October 15). During the strong mixing event, the model underestimated bottom temperature by about 2^{o}C and underestimated bottom salinity by about 1 psu. The reason for such discrepancies is unclear.

In Cruise II, the glider was deployed at mid-shelf, about 100 km northeast of Pulley Ridge in late winter of 2012 (blue track in Fig. 1). The glider was directed along the opposite course to Cruise I as it traveled from the mid-shelf westward toward the shelf edge. Once crossing the 70 m isobath, it turned south and took a steady path toward Pulley Ridge following the 70-75 m isobaths before circling Pulley Ridge for a couple of weeks at the end of the deployment. Overall, modeled temperature and salinity values showed similar ranges and vertical structures as those measured by the CTD on the glider (not shown).

3.2. CTD profiles

We also compared the model results against CTD profiles collected during Cruise I (Fig. 4). For illustration purpose, we selected two stations (stations 2 and 9) as a representation of water properties in the Pulley Ridge region, and two stations (stations 14 and 18) over Pourtalès Terrace in the southern Florida Straits. Generally, the modeled temperature agreed very well with the data (Fig. 4a-d). The model slightly underestimated the salinity but modeled salinity profiles were generally in agreement with observations. In particular, both the model and observed salinities showed a subsurface maximum between 40-120 m, which was likely from the LC subsurface water (Paluszkiewicz et al., 1983; He and Weisberg, 2003).

3.3. Sea surface height

In order to examine the impacts of the LC/FC on the shelf and the shelf break, it is critical to verify the frontal location of the LC/FC during the model period. Here we use SSH data derived from the AVISO delayed real-time products (http://aviso.com/). We have compared daily SSH and gradients of SSH from both the model and AVISO satellite data. An example of the comparison is shown here. Fig. 5 compares the modeled and observed SSH along a north-south transect (83.7^{o}W, purple line in Fig. 1), which crosses the Florida Straits and the Pulley Ridge region. Because there was an offset of about 0.5 m between the modeled and AVISO SSH due to a difference in reference plane, we have removed the mean SSH for the comparison. Both the modeled and the satellite SSH showed a strong biweekly to seasonal north-south migration in the FC front, likely due to the propagation of baroclinic Rossby waves (e.g., Hurlburt and Thompson, 1982). In order to further quantify the correlation between modeled and observed FC frontal meandering, we defined the front of the FC as the location of maximum SSH gradient (northern flank) and computed the correlation coefficient between the modeled and the observed FC front. The resulting coefficient was 0.72 (p<0.001) for the model period, indicating a strong correlation. Both modeled and AVISO SSH also indicated that there was a strong and prolonged northward migration in the FC front during July-November, 2012, which had significant impacts on the Pulley Ridge circulation (see discussion in section 4).

3.4. Quantitative model skills

In order to further assess the model performance, we quantified the degree of model-data agreement through various quantitative metrics. A point-to-point scatter plot between model results and data including the glider, Argo float, CTD casts and GOMECC2 bottle data is presented in Fig. 6 with associated metrics (defined below). The standard correlation coefficient (CORR) measures the linear correlation between the observed values and corresponding model results at the measurement time and locations (e.g. Edwards, 1976):

$$CORR = \frac{\frac{1}{N}\sum_{i=1}^{N}\left[\xi_{model}(i) - \overline{\xi}_{model}\right]\left[\xi_{obs}(i) - \overline{\xi}_{obs}\right]}{\sigma_{model}\sigma_{obs}} \quad (1)$$

where ξ_{obs} is the observed value, ξ_{model} is the modeled value at the sampling location, N is the number of samples. σ_{obs} and σ_{model} are the standard deviations of the observations and corresponding model results, respectively.

The root-mean-squared deviation (RMSD) measures the standard deviation between the observations and corresponding model results, defined as (e.g., Pan, 2012; Pan et al., 2014; Criales et al., 2015):

$$RMSD = \sqrt{\frac{\sum_{i=1}^{N}\left[\xi_{model}(\mathrm{i}) - \xi_{obs}(\mathrm{i})\right]^2}{N}} \quad (2)$$

Another metric is the so-called mean bias (BIAS), which measures the mean difference between the observed and corresponding modeled values (e.g., Pan et al., 2011):

$$BIAS = \frac{\sum_{i=1}^{N}\left[\xi_{model}(\mathrm{i}) - \xi_{obs}(\mathrm{i})\right]}{N} \qquad (3)$$

The computed results of these metrics are shown along with the point-to-point scatter plot (Fig. 6). Consistent with the qualitative comparisons above, model temperature agreed with data throughout the water column very well (CORR=0.94, RMSD=1.04 ^{o}C, BIAS=0.05 ^{o}C) (Fig. 6a). Modeled salinity was also generally in agreement with data (CORR=0.91, RMSD=0.28 psu) (Fig. 6b). A significant deviation, however, existed (BIAS=-0.19 psu), which can also be seen in the comparison of salinity profiles (Fig. 4). This highlights the difficulty in pinpointing the exact locations of the various water masses both horizontally and vertically. These discrepancies between model results and data may be attributed to various factors, such as the inaccurate boundary conditions, surface freshwater fluxes, and numerical deficiencies (e.g. shallower mixed layer predicted).

4. Results and Discussion

4.1. Impacts of the LC/FC frontal position on the cross-shelf transport

As seen from the AVISO and modeled SSH (Fig. 5), the position of the core FC in the southern Florida Straits migrates strongly in the north-south direction, which is consistent with previous studies (e.g., Mooers and Fiechter, 2005; Kourafalou et al., 2012). Here we will show how this migration might impact the Pulley Ridge region. For this purpose, we examined several representative examples of modeled currents superimposed on the temperature field at 50 m depth (Fig. 7). On April 03, 2011, the LC flowed from north to south before transiting to the FC, and made an almost 90^{o} turn toward the northeast at the entrance of the Florida Straits (Fig. 7a). The northern front of the LC/FC impinged upon the shelf slope south of Pulley Ridge. Widespread relatively cold Gulf slope water (temperature ~ 19-20^{o}C) can be seen in the vicinity of the Pulley Ridge region. In the second example, about two months later on May 27, the LC flowed southeast into the Florida Straits with its northern front flushing the southern Pulley Ridge area. This kind of water intrusion from the Gulf is likely due to the closeness of the LC/FC to the shelf break, which leads to the spillover of the Gulf waters at the southwest corner of the shelf.

Another example of on-shelf intrusion associated with the migration of the LC/FC front is shown in Fig. 7c. On July 1, 2011, the northern front of LC/FC moved on top of the continental slope south of Pulley Ridge, closely hugging the shelf and completely blocking the northern Gulf water from entering the Florida Straits. A meso-scale eddy was formed over the western slope between the LC/FC front and the shelf edge, which drove a cross-shelf transport along the southern edge of the eddy. In this case, some of the intruded water appeared to make a southward turn on the shelf and continued across the shelf break to rejoin the LC/FC. We will further discuss the formation of the eddy at this location and the associated impacts on the Pulley Ridge region in section 4.2. As a contrasting example, we show a case in which the LC/FC front retreated southward on September 1, 2011, such that its northern front was not in contact with the shelf slope (Fig. 7d). In this case, there was no on-shelf transport of the Gulf waters.

The intrusions of Gulf water in the first three cases covered the entire southern Pulley Ridge area where the mesophotic coral reefs are located. Therefore such intrusions might have a significant impact on the local water properties in this area. Based on these examples, we hypothesized that on-shelf transport of Gulf water on Pulley Ridge is closely related to the frontal position of the LC/FC system. To quantify the cross-shelf transport associated with these intrusion, we calculated the depth-averaged on-shelf volume transport along the 83.7^{o}W transect (purple line in Fig. 1), only for the shelf portion (Fig. 8a). The transport was defined for every grid surface (y-z plane) as depth-integrated water flux multiplying the grid size in y-direction (unit: Sv=10^6 m^3/sec). By definition, the local maxima of the frontal position in the resulting time series indicated the northernmost position of the FC northern front. Over the two-year model period, there were five events when the FC front approached the shelf edge (Fig. 8b): 1) June 05 – July 12, 2011; 2) November 18 – December 6, 2011; 3) January 20-31, 2012; 4) June 4 - October 08, 2012; 5) October 27 – November 29, 2012. During each of these events, there was significant corresponding on-shelf transport near southern Pulley Ridge (Fig. 8a) with the exception of the second event, when there was strong off-shelf transport between 25.6-26.0^{o}N. During the rest of the events, the on-shelf transport was broad and strong with the flux at the southern shelf edge being greater than 0.01 Sv (depth average speed ~ 10 cm sec^{-1}). The on-shelf transport also extended far north, reaching 26^{o}N. During the second event (November 18 – December 6, 2011), model results showed an anti-cyclonic eddy on top of the shelf break between 25.0-26.0^{o}N, causing on-shelf transport in the north (~between 25.6-26.0^{o}N), yet off-shelf transport in the south (25.0-25.6^{o}N). There were some other relatively weaker events when the FC front also migrated northward approaching the slope (e.g. April 12-19, 2011 or August 10-20, 2011), during which significant, but generally weaker, eastward cross-shelf transport was also evident. Between these events, the cross-shelf transport was generally weak except during October 15, 2011 - January 25, 2012, when there was strong off-shelf transport that covered much of the southern Pulley Ridge area with the volume reaching 0.01 Sv.

Quantitatively, there was a strong correlation between the FC frontal position and the on-shelf transport (Fig. 9), which was positive in the south between 24.7-25.3^{o}N and negative in the north (>25.4^{o}N). In particular, the correlation coefficient had a maximum of 0.70 at shelf edge ~ 24.7^{o}N, and gradually decreased northward. In general, because the eastward transport often starts in the north and propagates to the south (e.g., Fig. 8a), there is a time-lag between the transport at the north and at the south, causing the negative correlation in this region (not shown).

The exact mechanism driving the on-shelf transport over the southern Pulley Ridge is not entirely clear, but one possible mechanism is the geostrophic adjustment. When the northern front of the LC approaches the southern Pulley Ridge, a pressure gradient is formed pointing to the north due to the higher SSH of the LC. To balance this pressure gradient, an on-shelf current is then developed with a companion Coriolis force pointing to the south, balancing the pressure gradient. When the LC front retreats to the south, the sea level gradient at the shelf edge becomes small, and the on-shelf current thus diminishes or ceases to exist.

4.2. Meso-scale eddy and deep water upwelling

The instability of the LC/FC produces numerous filaments and frontal eddies in the Gulf of Mexico. Abundant literature can be found regarding the mechanisms of LC/FC frontal eddy generation (e.g., Vukovich and Maul, 1985; Biggs et al., 1996; Oey et al., 2005; Cherubin et al., 2006; Rudnick et al., 2015). One prominent example is the so-called Tortugas Eddy, a nearly stationary meso-scale eddy occupying a large area at the entrance of the Florida Straits with its northern flank overlaying over the slope south of Pulley Ridge (e.g., Fratantoni et al. 1998; Lee et al., 1995). Here we focus on the eddy activities over the western slope off the southern Pulley Ridge area with the purpose of understanding the potential upwelling of cold deep waters onto the shelf.

There are two scenarios in which we may find an eddy in this area: 1) an eddy passing through the area, and 2) an eddy is locally generated. The first scenario has been discussed by many literatures, in which frontal eddies regularly form at the vicinity of the LC in the gulf and gradually move downstream with the LC into the Florida Straits (e.g., Oey et al., 2005; Liu et al., 2011; Le Hénaff et al., 2012). We are therefore not discussing this scenario further, although it is worth mentioning that when the frontal eddies approaches Pulley Ridge, they can be blocked by the LC/FC front from moving in the Florida Straits. Kourafalou and Kang (2012) discussed the mechanism of LC/FC blocking eddies from entering the Florida Straits, using a HYCOM model.

As an example of the second scenario, Fig. 10a-e presents another case of eddy evolution in this area (July 9-August 03, 2012). During this period, the LC/FC front at the entrance of the Florida Straits was in contact with the shelf break south of Pulley Ridge, whereas its upstream (LC) arm was largely in parallel with but about 40 km away from the western shelf break. Therefore the slope water was nearly completely blocked by the LC/FC. A small portion of the LC came in contact with the slope and turned north becoming a northward flow along the continental slope (Fig. 10a). This flow and the southward LC formed an elongated low shear zone with low temperature at the center. A few days later (July 16), an eddy was formed locally west of the southern Pulley Ridge area, centering at around (25.0^{o}N, 84.2^{o}W) (Fig. 10b). There seemed to be a second eddy further north centering at (26.5^{o}N, 84.3^{o}W). By July 21, the northern eddy became elongated and moved southward in contact with the Pulley Ridge eddy (Fig. 10c). On July 25, the two eddies merged together, forming a new eddy with the center at (25.1^{o}N, 84.4^{o}W). The temperature at the center of the Pulley Ridge eddy had been decreasing slowly during this period before the merge with the other eddy. In addition, the Pulley Ridge eddy also seemed to have entrained some cold water onto the shelf (Fig. 10b-d). The new eddy stayed at the same location for another two week. Cold water remained visible on the northeastern side of the eddy (Fig. 10e).

The low temperature at the center and eastern flank of the Pulley Ridge eddy indicated strong upwelling. To further understand this, we plotted the temperature and currents along a cross-shelf transect at 25.0^{o}N where the eddy center was located most of the time (Fig. 11). On July 9, the eddy started to form and the associated vertical velocity field along the transect showed no sign of upwelling (Fig. 11a). On July 16, the eddy had fully formed and the vertical velocity field showed strong divergence at the eddy center (Fig. 11b). In the meantime, the 22^{o}C isotherm near the center of the eddy was lifted to 40 m. By July 21, the eddy center moved closer to the shelf break at about 84.2^{o}W and an enclosed cell was formed over the upper slope between 50-150 m (Fig. 11c). Strong divergence can be found along the western edge of the eddy that brings cold deep water to the base of thermocline. On July 25, when the two eddies merged, the center of the merged eddy was somewhat twisted westward to 84.4^{o}W, but the eastern wing of the eddy remained in contact with the slope (Fig. 10d). Significant upwelling at 84.2^{o}W remained, suggesting that the upwelling does not necessarily occur at the center of the eddy. Note that during this period, the 22^{o}C isotherm extended onto the shelf to the 50 m isobaths, passing through the Pulley Ridge region. The upwelling on the eastern side of the new eddy continued (Fig. 11e) until the eddy dissipated on August 16.

To quantify the relationship between eddy activities and upwelling, we computed the mean vertical velocity within a "control volume" as defined horizontally by the purple box in Fig. 10b with a vertical depth range of 50-300 m. The resulting vertical velocity was further low-pass filtered with a 52-hour filter. In this way, the impacts of potential high frequency oscillations of the flow field (e.g., inertial oscillations) were effectively removed. We also calculated the mean

Okubo-Weiss (OW) parameter (Okubo, 1970; Weiss, 1991) in the control volume, which essentially represents the balance between the magnitude of the relative vorticity and deformation rate (e.g., Veneziani et al., 2005; Poje et al., 2010):

$$OW = d^2 - \zeta^2 \tag{4}$$

where ζ is the relative vorticity:

$$\zeta = \frac{\partial v}{\partial x} - \frac{\partial u}{\partial y} \tag{5}$$

d is the deformation rate:

$$d = \sqrt{\left(\frac{\partial u}{\partial x} - \frac{\partial v}{\partial y}\right)^2 + \left(\frac{\partial v}{\partial x} - \frac{\partial u}{\partial y}\right)^2} \tag{6}$$

The OW parameter is typically negative at the center of an eddy due to the high relative vorticity and positive around the eddy edge due to the high deformation rate. This property makes it very helpful in tracking eddies in the ocean (e.g., Isern-Fontanet et al., 2003; Cruz Gómez and Bulgakov, 2007; Kourafalou and Kang, 2012). As an example, the OW maps corresponding to the eddy evolution case above (July 09-August 03, 2012) are presented in Fig. 12a-e. The eddy formation and evolution near 25°N as well as merger with the northern eddy are all represented in the OW evolution maps, consistent with the flow field in Fig. 10.

A comparison of the mean vertical velocity and mean OW within the same control volume indicates a close correlation between the upwelling and the eddy activity (Fig. 12f). For example, during mid-July to mid-August, 2012, strong upwelling persisted in this area with an average vertical velocity ~ 4 m day^{-1}, which was closely correlated with the presence of the Pulley Ridge eddy noted above, as also indicated by the negative OW value. After mid-August, weak downwelling and upwelling rotated until mid-October. For the period of June-August 2012, the correlation coefficient between the mean vertical velocity and mean OW parameter within the control volume was -0.71 (p<0.001).

As noted above, the FC front tended to migrate strongly northward during the summer and fall period for both 2011 and 2012 (Figs. 7 and 10b). The northward migration in 2012, however, was much longer and further north than that in 2011. During this period, the FC northern front generally remained on top of the continental slope close to the Pulley Ridge-Tortugas shelf edge, blocking LC/FC frontal eddies from moving into the Florida Straits. At the same time, many eddies were born and disappeared locally at the southwestern corner of the shelf, similar to the evolution of the Pulley Ridge eddy shown in Fig. 10a-e. All of these could also have strong impacts on the deep water upwelling over the western slope of southern Pulley Ridge area.

However, both frontal movements (Figure 8) and eddy activities (Figures 10 and 11) can also affect shelf bottom temperature through other processes. Therefore the relationship between shelf bottom temperature with eddy activities or frontal movement is complex. To illustrate the influence of upwelling over the slope area on the shelf bottom waters, we compared the near-bottom temperature (referred as T-shelf hereafter) at a location (25^{o}N, 83.5^{o}W) over Pulley Ridge with the average temperature at 60m of the control box above (referred as T-slope hereafter) (Fig. 12g) along with the mean vertical upwelling velocity (W) and OW within the same control volume (Fig. 12f). Here we chose the period June-August 2012, which covered the eddies and upwelling events shown in Fig. 12a-e. The T-slope showed a clear and persistent decline for the period shown until August 3rd, 2012, likely responding to the persistent upwelling reflected in the generally positive W and negative OW. We note that negative OW can be derived from both cyclones and anti-cyclones. Most eddies in the area, however, are anti-cyclones during these periods. The T-slope, however, increased in early August when the upwelling was decreasing (W was still generally positive) for unclear reasons. Overall, there were strong correlations between T-slope, OW and W with r=0.64 ($p < 0.001$) for T-slope and OW and r=-0.61 ($p < 0.001$) for T-slope and W, respectively.

Consistent with the variability of T-slope, T-shelf also decreased in June-July 2012 and then increased in late July and August. The correlation coefficient between T-shelf and T-slope, however, was significant but low (r=0.26, $p<0.01$), suggesting weak influence of the slope waters through upwelling. Several factors may have contributed to the variability of T-shelf, including horizontal advection of the warm gulf waters onto the shelf in response to LC/FC frontal migration (e.g., Fig. 7b), and the cross-over onto the shelf of deep cold slope waters due to eddy-driven upwelling (e.g., Fig. 11). One of the consequences of the combining effect is the clear oscillatory behavior of T-shelf.

Other than the mechanism of upwelling triggered by eddy activities, we also considered a possible mechanism described by Roughan and Middleton (2004) and Marchesiello et al. (2000), in which upwelling could also happen within the bottom boundary layer (BBL) through Ekman transport in response to encroachment of strong along-shore currents. We compared the modeled near-bottom vertical velocities on the continental slope and the shelf break near Pulley Ridge against the estimated vertical bottom velocity due to along-shore current encroachment (equation 1 from Roughan and Middleton, 2004). We found that the modeled vertical velocities and estimated vertical velocities, however, were too small to account for the mean upwelling velocity of the control volume in Fig. 10b. In addition, no correlation was found between the estimated vertical velocities due to current encroachment and the mean vertical velocities of the control volume. Given the negative relationship between the upwelling and the OW number in Fig. 12f, we conclude that the upwelling over the slope in the above case was closely related to eddy activities rather than along-shore current encroachment.

These upwelling events triggered by eddies or LC/FC frontal movement may have significant impact on southern Pulley Ridge habitats. In recent ROV benthic surveys of Pulley Ridge HAPC, Reed et al. (2016) found an extreme loss of coral cover over the last decade or so. The average hard coral cover decreased by 92.8% between 2003-2013 (Reed et al., 2014; Reed, 2016). However, in 2014, additional surveys to the west of the Pulley Ridge HAPC discovered high densities of relatively young coral recruits. On a possible positive note, a large number of these corals are relatively new recruits. So it appears that the coral is growing back from whatever die-off occurred between 2003 and 2013. Whether these upwelling events are cold enough to negatively impact the coral is unknown at this time. The cooling events simulated by this model (about 22^{o}C) were not low enough to kill or bleach the coral, which is about 18^{o}C. However, we are not ruling out the possibility of upwelling water with lower temperature in other years without further examination.

4.3. A shelf-edge return flow between the Pulley Ridge and Florida Keys

Model results indicate frequent presence of a westward jet along the shelf break from Florida Keys to Pulley Ridge with a magnitude of more than 40 cm sec^{-1} during late fall and early winter period of both 2011 and 2012. Here first we briefly describe the time evolution of the jet using the results in 2011. The jet appeared to start on October 18, 2011, when the FC impinged on western Florida Keys. Between the front of the FC and the shelf break, a small cyclonic eddy formed near the Dry Tortugas with a diameter of about 70 km (Fig. 13a). As the eddy moved downstream and, at the same time, getting closer to the shelf break, a clear westward flow can be seen along the northern edge (shelf break) of the eddy with a velocity of about 15 cm sec^{-1} (Fig.

13b). The eddy began to dissipate on October 22, while the westward flow remained along the shelf edge, only becoming stronger with the western end turning north, largely following the 60 m isobath to intrude the southern Pulley Ridge (Fig. 13c). Once on the shelf, the jet became a more broad current. This jet persisted in the next several weeks and its northern leg extended further northward into Pulley Ridge (Fig. 13d).

It appears that the origin of the return jet is closely tied to the impinging point of the FC with the shelf, so it also moves east or west when the FC meanders. Lee et al. (1995) also documented the along-shore westward flow and the eastward movement of its origin point. They suggested, however, that the westward flow was closely tied to the eastward translation of the Tortugas Eddy.

The relationship between eddies near Dry Tortugas with the jet can be better illustrated with the OW parameter, which indicated that the initiation of the jet appeared to be closely associated with eddies (Fig. 13e-f). Further, the demise of these eddies might have strengthened the jet (Fig. 13g-h). When the jet became stronger, it was represented by a narrow band with high but patchy OW value along the path of the jet. The exact role and mechanism of these eddies in the formation and evolution of this jet, however, remain unclear.

To further verify the existence of this return flow, here we present a comparison of the model results with historical observations from a current meter deployed on the outer edge of Looe Key (24.54^{o}N, 81.40^{o}W) in 1986-1988 (Fig. 14). The water depth of the mooring station was 32 m, and the current meter was fixed at 14 m below the surface. Only two segments (October 09, 1986 - January 07, 1987 and September 04, 1987 - March 29, 1988) of data are available, both of which were during fall-winter periods when the modeled return flow was most prominent. Therefore the comparison was indirect. The model results at the same location and depth as the current meter were extracted for the comparison. Both data and model results were filtered with a 72-hour low-pass filter, and only the E-W component was shown. The N-S component is quite weak (<5 cm sec^{-1}) at this location because the topography is aligned largely in the west-east direction.

Overall, both the model results and observations showed oscillatory currents but also prolonged periods of persistent westward flow (Fig. 14). Both model and observed east-west velocities were <0.5 m s^{-1}. The observed E-W velocity had an average value of -0.04±0.14 m s^{-1} and -0.01±0.19 m s^{-1} for 1986-87 and 1987-88 segments, respectively. Modeled E-W velocity had a mean -0.05±0.14 m s^{-1}, similar to the observed values. On a closer examination of the spectra for the model results and observations, both model and observed currents showed persistent westward flow that lasted from a few days to about two weeks. These included mooring periods in October 30 – November 16, 1986 and September 20 – December 12, 1987, as well as model periods in November 02 – 17, 2011 and December 05 – 16, 2011. Furthermore, this station is on the northern edge of the return flow (see below), and hence it is reasonable that the average current is quite weak.

The similarities between modeled and observed currents at this location support the modeled return flow along the Florida Keys. In fact, the presence of this jet is a well-documented phenomenon, although its dynamic mechanism is not yet fully understood (e.g., Lee et al., 2002; Kourafalou et al., 2006; Kourafalou et al., 2009). Previous studies largely attributed the cause of the return flow near the Florida Keys to the prevailing northeasterly winds during this time of the year (Lee et al., 2001; Kourafalou et al., 2006). Such a mechanism, however, did not explain the bottom trapped-wave feature of this jet (see below). Oey and Zhang (2004) described another scenario that along-slope return jet, at much deeper water, can be generated when the LC eddies interact with the continental slope of the West Florida Shelf. No previous studies, however, had reported a (northward) continuation of the jet through the southern Pulley Ridge.

To test the effect of the surface winds on the return flow, we turned off the winds (setting wind stresses to zero) in the model between October 13 and November 25, starting about one week before the appearance of the jet on October 20, 2011. During this period, the surface winds were predominantly northeasterly, and may contribute to westward flow near the surface. This was confirmed by the comparison between the two simulations, which indicated a similar but weaker westward jet in the case of without surface winds (Fig. 15). At 50m depth, the velocity reduction was about 15%. The geographic extent covered by the jet seemed to be smaller as well. The origin location of the jet, however, seemed to be the same, also tying to the contact point of the FC with the shelf (Fig. 15 a, d). These results indicate that the main driver of the jet is likely the shelf impingement of the FC owing to its meandering. Lee et al. (2002) suggested that the southward movement of the FC can lead to the strengthening of the westward flow due to more persistent eddies near Dry Tortugas.

Further evidence of the impacts of surface winds is from the vertical structure of the jet along a cross-transect through the Dry Tortugas along 83^{o}W (Fig. 16). In both cases, it is clear that this jet is a narrow jet, which exists largely at the shelf edge with a width around 10 km on initiation and extends much deeper to about 150m over the slope with a width about 30km as it becomes stronger (> 50 cm sec^{-1}). Without surface winds, however, the jet became much weaker, suggesting that wind-driven transport indeed enhances the jet near the surface. The westward transport through the cross-transect was about 16% less when there is no surface wind forcing, which is consistent with the aforementioned velocity reduction.

The return flow may bring slope water onto Pulley Ridge which could be important for the connectivity of benthic and fish species between Pulley Ridge and the Florida Keys/Tortugas (e.g., Cowen and Sponaugle, 2009). It is thought that the gene flow would be from Pulley Ridge towards Keys (Vaz et al., 2016), but the westward return flow shows how genes from the Keys could also move westward and back to Pulley Ridge. These results are thus critical for better understanding of the connectivity between mesophotic and shallow reefs (Vaz et al., 2016).

5. Conclusions

A high-resolution regional ocean model based on ROMS was developed for the southern Florida Shelf and Florida Straits region. A two-year (2011-12) simulation was conducted and the model results were generally in good agreement with available satellite and *in situ* data. The model was also capable of reproducing the major known physical features in this area. We have used this model to investigate the potential impacts of the LC/FC on the shelf circulation and water properties over the Pulley Ridge.

Our analysis suggests that the meandering of the LC may exert strong impacts on the circulation dynamics over Pulley Ridge. In particular, the north-south migration of the LC/FC front is usually accompanied with a west-east cross shelf transport along the western shelf edge of Pulley Ridge. Strong on-shelf transport may take place, when the FC northern front is close to the shelf edge at the southern end of Pulley Ridge. Moreover, cross-shelf transport typically starts from the north with an increasing time-lag to the south.

Our model results also reveal frequent generation and propagation of meso-scale cyclonic eddies along the western Florida slope throughout the modeling period, consistent with previous studies (e.g. Kourafalou and Kang, 2012). These eddies can be generated upstream in the Gulf, then propagating southward alongside with the LC, or locally over the western slope of the southern Pulley Ridge. In both cases, these eddies could be trapped around the southwestern corner of the shelf slope by the LC/FC front when it is in close contact with the shelf break, in some cases without being able to enter the Straits during their entire life cycle (days to weeks) (Kourafalou and Kang, 2012). Our analysis further suggests that these cyclonic eddies may drive strong upwelling of cold and nutrient-rich slope waters at the eddy center or along northeastern edge. The upwelled waters sometimes cross the shelf break and intrude about 20-30 km into the shelf. The temperature of upwelled waters during the model period was higher than 21^{o}C, higher than the criterion for coral bleaching (Reed et al. 2016). However, we can’t rule out the possibilities of lower temperature water being upwelled and hence significantly impacting the Pulley Ridge habitat and fauna during other times.

Our results also indicate that an intermittent westward narrow jet with a width of 10-30 km exists along the shelf edge between the Florida Keys and Pulley Ridge during late fall and early winter. A comparison with historical current measurements (1986-87) from a mooring station off Looe Key in the Florida Keys yielded similar statistics of the current, although no direct comparison was possible without measurements for the model period. This result is consistent with results from previous studies (Lee et al., 2002; Kourafalou et al., 2006; Kourafalou et al., 2009). A close examination of the evolution of the jet and the results of a numerical experiment suggest that this jet is likely a result of the FC impinging upon the shelf and hence blocking the slope water from further going downstream. Consistent with previous studies, the typical northeasterly winds during this time of the year generally enhance the jet. Our results, however, show that surface winds are not the determining factor for the generation of this return flow. Although the formation mechanism of this jet is yet to be determined, it is certainly of importance for further understanding the connectivity between the mesophotic reefs in Pulley Ridge and shallow reefs in the Tortugas area.

Acknowledgements

We acknowledge the funding support for the Bluefin Spray Glider missions by the Battelle Memorial Institute. We would like to thank Dr. Laurent Cherubin at HBOI for helping with the initial model setup and insightful advices. We thank Dr. Bing Ouyang, Dr. Anni Vuorenkoski and Mr. Andrew Krupski for calibrating, processing and providing the glider data. We thank Dr. Ned Smith at HBOI-FAU for providing the mooring data for the Florida Reef Tract. We also thank Dr. Robert Weisberg, Dr. Lianyuan Zheng and Dr. Yonggang Liu from University of South Florida (USF) for helpful discussions. HYCOM data was downloaded from website: http://tds.hycom.org/. The blended SST satellite data were obtained from the Physical Oceanography Distributed Active Archive Center (PO.DAAC, http://podaac.jpl.nasa.gov) at the NASA Jet Propulsion Laboratory, Pasadena, CA. The satellite SSH was produced and distributed by AVISO (http://www.aviso.altimetry.fr/). The Argo Float data was downloaded from website: http://www.argo.ucsd.edu. The river discharge data was from the USGS (http://waterdata.usgs.gov/nwis). The MODIS Chlorophyll image was provided by Dr. Chuanmin Hu at USF. We gratefully acknowledge the support of NOAA Cooperative Institute for Ocean Exploration, Research, and Technology (CIOERT) at Harbor Branch Oceanographic Institute, Florida Atlantic University for the field survey. The crews of the NOAA ship R/V *Nancy Foster* and the University of Connecticut's *Kraken 2* ROV are thanked for their support. CIOERT gratefully acknowledges funding provided by the NOAA Office of Ocean Exploration and Research (OER Award #: NA09OAR4320073), NOAA Deep Sea Coral Research and

Technology Program, and NOAA Office of Marine and Aviation Operations (OMAO) in support of the research, ship operations, and ROV operations. This is HBOI-FAU Contribution Number 2053.

References

Biggs, D.C., Fargion, G.S., Hamilton, P., Leben, R.R., 1996. Cleavage of a Gulf of Mexico loop current eddy by a deep water cyclone. J. Geophys. Res. 101, 20,629–20,641. doi:10.1029/96JC01078.

Chassignet, E.P., Hurlburt, H.E., Metzger, E.J., Smedstad, O.M., Cummings, J.A., Halliwell, G.R., Bleck, R., Baraille, R., Wallcraft, A.J., Lozano, C., Tolman, H.L., Srinivasan, A., Hankin, S., Cornillon, P., Weisberg, R.H., Barth, A., He, R., Werner, F., Wilkin, J., 2009. US GODAE: global ocean prediction with the HYbrid Coordinate Ocean Model (HYCOM). Oceanography 22, 64-75. doi: 10.5670/oceanog.2009.39.

Cherubin, L. M., Morel, Y., Chassignet, E. P., 2006. Loop Current ring shedding: The formation of cyclones and the effect of topography. J. Phy. Oceanog. 36(4), 569-591.

Cowen, R. K., Sponaugle, S., 2009. Larval Dispersal and Marine Population Connectivity. Annual Review of Marine Science 1(1), 443-466. doi: 10.1146/annurev.marine.010908.163757

Criales, M.M., Cherubin, L.M., Browder, J.A., 2015. Modeling Larval Transport and Settlement of Pink Shrimp in South Florida: Dynamics of Behavior and Tides. Marine and Coastal Fisheries 7, 148-176. doi: 10.1080/19425120.2014.1001541.

Cross, V., Twichell, D.C., Halley, R.B., Ciembronowicz, K.T., Jarrett, B.D., Hammar-Klose, E.S., Hine, A.C., Locker, S.D., Naar, D.F., 2005. GIS compilation of data collected from the Pulley Ridge Deep Coral Reef region. USGS Open-File Report 2005-1089, Reston, VA.

Davis, R.E., Eriksen, C.C., Jones, C.P., 2002. Autonomous buoyancy-driven underwater gliders, in: Griffiths, G. (Ed.), The Technology and Applications of Autonomous Underwater Vehicles. Taylor and Francis, London, pp. 37-58.

Davis, R. E., Regier, L. A., Dufour, J., Webb, D. C., 1992. The Autonomous Lagrangian Circulation Explorer (ALACE). J. Atmosph. and Oceanic Tech. 9(3), 264-285.

Edwards, A.L., 1976. The correlation coefficient, in: An Introduction to Linear Regression and Correlation. W. H. Freeman & Company, San Francisco, CA, pp. 33-46.

Fratantoni, P.S., Lee, T.N., Podesta, G.P., Muller-Karger, F., 1998. The influence of Loop Current perturbations on the formation and evolution of Tortugas eddies in the southern Straits of Florida. J. Geophys. Res. 103, 24759-24779. doi: 10.1029/98JC02147.

Gilbert, P.S., Lee, T.N., Podesta, G.P., 1996. Transport of anomalous low-salinity waters from the Mississippi River flood of 1993 to the Straits of Florida. Cont. Shelf Res. 16, 1065-1085. doi: 10.1016/0278-4343(95)00056-9.

Halley, R.B., Garrison, V., Ciembronowicz, K., Edwards, R., Jaap, W., Mead, G., Earle, S., Hine, A.C., Jarret, B., Locker, S., 2003. Pulley Ridge: the United States' deepest coral reef. USGS Open-File Report 03-54, Reston, VA.

He, R., Weisberg, R.H., 2003a. A loop current intrusion case study on the West Florida Shelf. J. Phys. Oceanogr. 33, 465-477. doi: 10.1175/1520-0485(2003)033<0465:ALCICS>2.0.CO;2.

He, R., Weisberg, R.H., 2003b. West Florida shelf circulation and temperature budget for the 1998 fall transition. Cont. Shelf Res. 23, 777-800. doi: 10.1016/S0278-4343(03)00028-1.

Hetland, R.D., Hsueh, Y., Leben, R.R., Niiler, P.P., 1999. A loop current-induced jet along the edge of the West Florida Shelf. Geophys. Res. Lett. 26, 2239-2242. doi: 10.1029/1999GL900463.

Hine, A.C., Halley, R.B., Locker, S.D., Jarrett, B.D., Jaap, W.C., Mallinson, D.J., Ciembronowicz, K.T., Ogden, N.B., Donahue, B.T., Naar, D.F., 2008. Coral Reefs, Present and Past, on the West Florida Shelf and Platform Margin, in: Riegl, B.M., Dodge, R.E. (Eds.), Coral Reefs of the USA. Springer, Dordrecht, pp. 127-173.

Hu, C., Nelson, J.R., Johns, E., Chen, Z., Weisberg, R.H., Müller-Karger, F.E., 2005. Mississippi River water in the Florida Straits and in the Gulf Stream off Georgia in summer 2004. Geophys. Res. Lett. 32, L14606. doi: 10.1029/2005gl022942.

Huh, O.K., Wiseman, W.J., Rouse, L.J., 1981. Intrusion of loop current waters onto the West Florida continental shelf. J. Geophys. Res. 86, 4186-4192. doi: 10.1029/JC086iC05p04186.

Hurlburt, H.E., Thompson, J.D., 1982. The dynamics of the Loop Current and shed eddies in a numerical model of the Gulf of Mexico. Elsevier Oceanography Series, 34, 243-297.

Kourafalou, V.H., Balotro, R.S., Peng, G., 2006. Seasonal Variability of Circulation and Salinity Around in Florida Bay and the Florida Keys: SoFLA-HYCOM Results and Comparison to In-situ Data. RSMAS technical report 2006-04, University of Miami, Miami.

Kourafalou, V.H., Peng, G., Kang, H., Hogan, P.J., Smedstad, O.-M., Weisberg, R.H., 2009. Evaluation of global ocean data assimilation experiment products on South Florida nested simulations with the Hybrid Coordinate Ocean Model. Ocean Dyn. 59, 47-66. doi: 10.1007/s10236-008-0160-7.

Kourafalou, V.H., Kang, H., 2012. Florida Current meandering and evolution of cyclonic eddies along the Florida Keys Reef Tract: Are they interconnected? J. Geophys. Res. 117. doi: 10.1029/2011JC007383.

Le Hénaff, M., Kourafalou, V. H., Morel, Y., Srinivasan, A., 2012. Simulating the dynamics and intensification of cyclonic Loop Current Frontal Eddies in the Gulf of Mexico, J. Geophys. Res. 117. doi:10.1029/2011JC007279.

Le Hénaff, M., Kourafalou, V. H., 2016. Mississippi waters reaching South Florida reefs under no flood conditions: synthesis of observing and modeling system findings, Ocean Dynamics, 66, 435-459. doi:10.1007/s10236-016-0932-4.

Lee, T.N., Leaman, K., Williams, E., Berger, T., Atkinson, L., 1995. Florida Current meanders and gyre formation in the southern Straits of Florida. J. Geophys. Res. 100, 8607-8620. doi: 10.1029/94JC02795.

Lee, T. N., Smith, N., 2002. Volume transport variability through the Florida Keys tidal channels. Cont. Shelf Res. 22, 1361-1377.

Lee, T.N., Williams, E., Johns, E., Wilson, D., Smith, N.P., 2002. Transport processes linking south Florida coastal ecosystems, in: Porter, J.W., Porter, K.G. (Eds.), The Everglades, Florida Bay, and Coral Reefs of the Florida Keys: An Ecosystem Sourcebook. CRC, Boca Raton, pp. 309-342.

Li, Z., Chao, Y., McWilliams, J.C., Ide, K., 2008. A three-dimensional variational data assimilation scheme for the regional ocean modeling system. J. Atmos. Oceanic Technol. 25, 2074-2090. doi: 10.1175/2008JTECHO594.1.

Liu, Y., Weisberg, R.H., 2012. Seasonal variability on the west Florida shelf. Prog. Oceanogr. 104, 80-98. doi: 10.1016/j.pocean.2012.06.001.

Liu, Y., Weisberg, R. H., Hu, C., Kovach, C. and RiethmüLler, R., 2011. Evolution of the Loop Current system during the *Deepwater Horizon* oil spill event as observed with drifters and satellites, in: Liu, Y., Macfadyen, A., Ji, Z.-G., and Weisberg, R.H. (Eds.), Monitoring and Modeling the Deepwater Horizon Oil Spill: A Record-Breaking Enterprise, American Geophysical Union, Washington, D. C., pp. 91-101. doi: 10.1029/2011GM001127.

Marchesiello, P., Gibbs, M.T., Middleton, J.H., 2000. Simulations of coastal upwelling on the Sydney continental shelf. Marine and Freshwater Res. 51(6), 577-88.

Mesinger, F., DiMego, G., Kalnay, E., Mitchell, K., Shafran, P.C., Ebisuzaki, W., Jović, D., Woollen, J., Rogers, E., Berbery, E.H., Ek, M.B., Fan, Y., Grumbine, R., Higgins, W., Li, H., Lin, Y., Manikin, G., Parrish, D., Shi, W., 2006. North American Regional Reanalysis. Bull. Am. Meteorol. Soc. 87, 343-360. doi: 10.1175/bams-87-3-343.Mooers, C.N., Fiechter, J., 2005. Numerical simulations of mesoscale variability in the Straits of Florida. Ocean Dyn. 55, 309-325. doi: 10.1007/s10236-005-0019-0.

Okubo, A., 1970. Horizontal dispersion of floatable particles in the vicinity of velocity singularities such as convergences. Deep sea research and oceanographic abstracts 17, 445-454. doi: 10.1016/0011-7471(70)90059-8.

Oey, L.-Y., Zhang, H.C., 2004. The generation of subsurface cyclones and jets through eddy–slope interaction. Cont. Shelf Res. 24, 2109-2131. doi: 10.1016/j.csr.2004.07.007.

Oey, L.-Y., Ezer, T., Lee, H.-C., 2005. Loop Current, rings and related circulation in the Gulf of Mexico: A review of numerical models and future challenges, in: Sturges, W., Lugo-Fernandez, A. (Eds.), Circulation in the Gulf of Mexico: observations and models. American Geophysical Union, Washington, D.C., pp. 31-56.

Paluszkiewicz, T., Atkinson, L.P., Posmentier, E.S., McClain, C.R., 1983. Observations of a loop current frontal eddy intrusion onto the West Florida Shelf. J. Geophys. Res. 88, 9639-9651. doi: 10.1029/JC088iC14p09639.

Pan, C., 2012. Application of a hybrid 3D-var data assimilation system in the Monterey Bay to study regional dynamics of the California Current System. The University of Southern Mississippi, Hattiesburg, Mississippi.

Pan, C., Yaremchuk, M., Nechaev, D., Ngodock, H., 2011. Variational assimilation of glider data in Monterey Bay. J. Mar. Res. 69, 331-346. doi: 10.1357/002224011798765259.

Pan, C., Zheng, L., Weisberg, R.H., Liu, Y., Lembke, C.E., 2014. Comparisons of Different Ensemble Schemes for Glider Data Assimilation on West Florida Shelf. Ocean Modelling 81, 13-24. doi: 10.1016/j.ocemod.2014.06.005.

Poje, A.C., Haza, A.C., Özgökmen, T.M., Magaldi, M.G., Garraffo, Z.D., et al., 2010. Resolution dependent relative dispersion statistics in a hierarchy of ocean models. Ocean Modelling 31(1), 36-50.

Prasad, T.G., Hogan, P.J., 2007. Upper-ocean response to Hurricane Ivan in a 1/25 nested Gulf of Mexico HYCOM. J. Geophys. Res. 112, C04013. doi: 10.1029/2006JC003695.

Reed, J.K., Farrington, S., Pomponi, S., Hanisak, D., Voss, J., 2012a. NOAA CIOERT cruise report: survey of the Pulley Ridge mesophotic reef ecosystem, NOAA Ship Nancy Foster, Florida Shelf-Edge Exploration II (FLoSEE) Cruise, Leg 1 - September 12-19, 2011. NF-11-09-CIOERT, http://data.nodc.noaa.gov/coris/library/NOAA/CRCP/other/non_crcp_publications/Deep-Sea/2011_Nancy_Foster_CIOERT_Cruise-

Leg_1_Preliminary_Cruise_Report_and_SEADESC_I_Report_2-29-2012_text_and_appendix.pdf.

Reed, J.K., Farrington, S., Harter, S., David, A., Shirley, P., 2012b. NOAA CIOERT cruise report: survey of the deep-sea coral and sponge ecosystem of Pourtales Terrace, NOAA Ship Nancy Foster, Florida Shelf-Edge Exploration II (FLoSEE) Cruise, Leg 2 - September 23-30, 2011. NF-11-09-CIOERT, http://data.nodc.noaa.gov/coris/library/NOAA/CRCP/other/non_crcp_publications/Deep-Sea/2011_Nancy_Foster_CIOERT_Cruise-Leg_2_Preliminary_Cruise_Report-w-Appendices_1-30-201.

Reed, J.K., Farrington, S., Moe, L.H., Harter, S., Hanisak, D., David, A., 2014. Characterization of the mesophotic benthic habitat and fish assemblages from ROV dives on Pulley Ridge and Tortugas during 2014 R/V Walton Smith cruise. NOAA CIOERT Cruise Report WS1412, http://www2.coastalscience.noaa.gov/publications/handler.aspx?resource=f3OonrEadpHqG3b8TbHyDjLSP/OBaDuGaZ1niq9ygew.

Reed, J.K., 2016. Pulley Ridge, Gulf of Mexico, USA, 23-25, in: Baker, E.K., Puglise, K.A., Harris, P.T. (Eds.), Mesophotic coral ecosystems - a lifeboat for coral reefs? The United Nations Environment Programme and GRID-Arendal, Nairobi and Arendal. 98 pp. ISBN: 978-82-7701-150-9. www.unep.org, www.grida.no.

Rivas, D., Badan, A., Ochoa, J., 2005. The Ventilation of the Deep Gulf of Mexico. J. Phys. Oceanog. 35(10), 1763-1781. doi: 10.1175/JPO2786.1.

Roughan, M., Middleton, J. H., 2004. On the East Australian Current: Variability, encroachment, and upwelling. J. Geophys. Res., 109, C07003. doi:10.1029/2003JC001833.

Rudnick, D.L., Davis, R.E., Eriksen, C.C., Fratantoni, D.M., Perry, M.J., 2004. Underwater gliders for ocean research. Mar. Technol. Soc. Bull. 38, 73-84. doi: 10.4031/002533204787522703.

Rudnick, D.L., Gopalakrishnan, G., Cornuelle, B.D., 2015. Cyclonic eddies in the Gulf of Mexico: Observations by underwater gliders and simulations by numerical model. J. Phys. Oceanogr. 45, 313-326. doi: 10.1175/JPO-D-14-0138.1.

Schofield, O., Kohut, J., Glenn, S., Morell, J., Capella, J., Corredor, J., Orcutt, J., Arrott, M., Krueger, I., Meisinger, M., 2010. A regional Slocum glider network in the Mid-Atlantic coastal waters leverages broad community engagement. Mar.Technol. Soc. 44, 64-74.

Shchepetkin, A.F., McWilliams, J.C., 2005. The regional oceanic modeling system (ROMS): a split-explicit, free-surface, topography-following-coordinate oceanic model. Ocean Modelling 9, 347-404. doi: 10.1016/j.ocemod.2004.08.002.

Umlauf, L., Burchard, H., 2003. A generic length-scale equation for geophysical turbulence models. J. Marine Res., 61(2), 235-265.

Vaz, A.C., Paris, C., Olascoaga, M.J., Kourafalou, V., Kang, H., Reed, J., 2016. The perfect storm: mis-match of bio-physical events drives larval reef fish connectivity between Pulley Ridge and the Florida Keys, Cont. Shelf Res., in review.

Veneziani, M., Griffa, A., Garraffo, Z.D., Chassignet, E.P., 2005. Lagrangian spin parameter and coherent structures from trajectories released in a high-resolution ocean model. J. Mar. Res. 63, 753-788. doi: 10.1357/0022240054663187.

Vukovich, F.M., Maul, G.A., 1985. Cyclonic eddies in the eastern Gulf of Mexico. J. Phys. Oceanogr. 15, 105-117. doi: 10.1175/1520-0485(1985)015<0105:CEITEG>2.0.CO;2.

Wang, Z.A., Wanninkhof, R., Cai, W.-J., Byrne, R.H., Hu, X., Peng, T.-H., Huang, W.-J., 2013. The marine inorganic carbon system along the Gulf of Mexico and Atlantic coasts of the United States: Insights from a transregional coastal carbon study. Limnol. Oceanogr. 58, 325-342. doi: 10.4319/lo.2013.58.1.0325.

Wanninkhof, R., Barbero, L., Byrne, R., Cai, W.-J., Huang, W.-J., Zhang, J.-Z., Baringer, M., Langdon, C., 2015. Ocean acidification along the Gulf Coast and East Coast of the USA. Cont. Shelf Res. 98, 54-71. doi: 10.1016/j.csr.2015.02.008.

Weisberg, R.H., Black, B.D., Yang, H., 1996. Seasonal modulation of the West Florida Continental Shelf Circulation. Geophys. Res. Lett. 23, 2247-2250. doi: 10.1029/96gl02184.

Weisberg, R. H., He, R., 2003. Local and deep-ocean forcing contributions to anomalous water properties on the West Florida Shelf, J. Geophys. Res., 108(C6), 3184, doi:10.1029/2002JC001407,.

Weisberg, R.H., He, R., Liu, Y., Virmani, J.I., 2005. West Florida shelf circulation on synoptic, seasonal, and interannual time scales, in: Sturges, W., Lugo-Fernandez, A. (Eds.), Geophysical Monograph Series. American Geophysical Union, Washington, D. C., pp. 325-347.

Weisberg, R.H., Zheng, L., Liu, Y., Murawski, S., Hu, C., Paul, J., 2014. Did Deepwater Horizon hydrocarbons transit to the west Florida continental shelf? Deep Sea Res. Part II. doi: 10.1016/j.dsr2.2014.02.002.

Weisberg, R.H., Zheng, L., Liu, Y., Lembke, C., Lenes, J.M., Walsh, J.J., 2014. Why no red tide was observed on the West Florida Continental Shelf in 2010. Harmful Algae 38, 119-126. doi: 10.1016/j.hal.2014.04.010.

Weisberg, R.H., Zheng, L., Peebles, E., 2014. Gag grouper larvae pathways on the West Florida Shelf. Cont. Shelf Res. 88, 11-23. doi: 10.1016/j.csr.2014.06.003.

Weiss, J., 1991. The dynamics of enstrophy transfer in two-dimensional hydrodynamics. Physica D: Nonlinear Phenomena 48, 273-294. doi: 10.1016/0167-2789(91)90088-Q.

List of Figure Captions

Fig. 1. Map of study area in the northeastern Gulf of Mexico, southwest Florida Shelf, and Florida Straits. The red rectangle = Pulley Ridge region on southwest Florida Shelf. Purple line indicates the N-S transect at 83.7^{o}W (approximate location of Pulley Ridge) for model verification and analysis. Light green polygons = Pulley Ridge Habitat Area of Particular Concern (PR HAPC). Purple polygons = Tortugas Ecological Reserves (TER). Black rectangle indicates model domain. Blue and red lines indicate Spray glider data from Cruise I and Cruise II, respectively. Cyan rectangles indicate CTD data from cruise GOMECC2 in 2012. Orange diamonds indicate CTD data from Cruise I. Orange number 2, 9, 14 and 18 indicate NOAA ship *Nancy Foster* CTD stations in Fig. 4. Green triangles indicate Argo Float data. Blue diamond indicates location of Florida Looe Key (LK) current mooring from HBOI-FAU. The black contour lines indicate bathymetry in meters.

Fig. 2. Glider track during Cruise I. Color indicates date. Black contours are isobaths in meters. Red polygons = PR HAPC. Purple polygons = TER.

Fig. 3. (a) Temperature profile observed from the glider versus (b) model temperature in 2011; (c) Salinity profile observed from the glider versus (d) model salinity in 2011.

Fig. 4: Temperature and salinity data obtained during Cruise I CTD casts versus model results at the same location and time. (a) – (d): temperature profiles at station 2, 9, 14 and 18; (e) – (h): salinity profiles at station 2, 9, 14 and 18.

Fig. 5. Time series of sea surface height along 83.7^{o}W (Fig. 1, purple line) from (a) AVISO satellite and (b) model.

Fig. 6. Point-to-point correlations between observed and modeled temperature (a) and salinity (b) below surface mixed layer (>50 m). Color indicates the sample depths.

Fig. 7. Model temperature (color) currents at 50 m depth on a) April 03, 2011; b) May 27, 2011; c) July 1, 2011; d) September 1, 2011. White contour lines are 70 m, 90 m, 100 m, 150 m, 200 m, 500 m, 1000 m, and 1500 m isobaths. Red polygons = PR HAPC. Purple polygons = TER.

Fig. 8. (a) Depth-integrated E-W volume transport through the cross-section along 83.7^{o}W (purple line in Fig. 1) and (b) corresponding FC northern frontal position (52 hour low-pass filtered). Blue shadows in (b) mark the five events when the LC approaches Pulley Ridge.

Fig. 9. Correlation coefficients and corresponding *p*-alues between the FC northern frontal position and the E-W volume transport along the western shelf edge from 24.6^{o}N to 26^{o}N. Purple dash lines are ±0.05 significant lines.

Fig. 10. An example of eddy trapped around the Pulley Ridge region on (a) July 09, 2012, (b) July 15, 2012, (c) July 21, 2012, (d) July 25, 2012 and (e) August 03, 2012. Color in (a) – (e) indicates temperature and vectors indicate currents at 50 m depth. White contour lines are 70 m, 90 m, 100 m, 150 m, 200 m, 500 m, 1000 m, and 1500 m isobaths. Red polygon denotes the location of PR HAPC. Purple box in (b) is the “control volume” area used for mean vertical velocity calculation. To reduce the strong contrast between the LC and shelf current,

all velocity vectors that is larger than 0.3 m/s are rescaled (the portion >0.3 m/s is multiplied by a factor 0.1), so that all the velocity vectors are brought to the velocity level near Pulley Ridge.

Fig. 11. Modeled temperature (color) and velocity (vectors) transect along 25^{o}N for the same dates in Fig. 10a-e. The vectors represent the combined currents in cross-slope and vertical directions. The vertical velocity is magnified 400 times to approximately represent the aspect ratio of the continental slope (depth increase 200 m corresponding to a horizontal distance of 80 km). Red arrows show the direction of current velocity. The red circle in (c) indicate the enclosed cell on the upper slope.

Fig. 12. Upper panel: Okubo-Weiss parameter for the respective velocity fields of the same dates in Fig. 10: (a) July 09, 2012, (b) July 15, 2012, (c) July 21, 2012, (d) July 25, 2012 and (e) August 03, 2012. Middle panel (f): mean vertical velocity (blue) and negative OW parameter (red) time series within the control volume (for 50-300m in depth) filtered by a 52 hour FFT low-pass filter. Lower panel (g): near-bottom temperature time series of the point at 56m depth on the shelf at 25^{o}N, 83.5^{o}W (blue line) and average temperature of the control box on the slope at 60m depth (red line) from June to August, 2012. The light blue areas in (f) and (g) highlight the period of the upwelling.

Fig. 13. Left: Temperature superimposed by velocity fields at 50 m depth on a) October 18, 2011; b) October 20, 2011; c) October 22, 2011; d) October 28, 2011. Right: Okubo-Weiss parameter for the respective velocity fields on the left panels: (e), (f), (g) and (h). Red arrows indicate wind direction and magnitude. White and gray contours are 70 m, 90 m, 100 m, 150 m, 200 m, 500 m, 1000 m, and 1500 m isobaths. Red and black polygons denote the location of PR HAPC. Green polygons denote the location of TER.

Fig. 14. (a) Blue dot indicates the location of the mooring station off Looe Key (LK) in the Florida Keys. (b) East-west velocity component of station data during October 9, 1986 – January 7, 1987. Positive numbers indicate eastward velocity and negative numbers indicate westward velocity. (c) East-west velocity of station data during September 4, 1987 – March 29, 1988. (d) Modeled east-west velocity at the same location during September 4, 2011 – March 29, 2012.

Fig. 15. Left: Temperature superimposed by velocity fields at 50 m depth on (a) 10/22/2011; (b) 11/10/2011; (c) 11/16/2011. Right: Same as left panel but from model run without wind stress: (d), (e) and (f). Red arrows indicate wind direction and magnitude. Purple arrows indicate the contact points of the FC with the shelf. White contours are 70 m, 90 m, 100 m, 150 m, 200 m, 500 m, 1000 m, and 1500 m isobaths. Red polygons denote the location of PR HAPC. Green polygons denote the location of TER. Blue current arrows indicate current speed larger than 0.3 m/s, while black current arrows indicate current speed smaller than 0.3 m/s.

Fig. 16. Zonal velocity field for the 83.7^{o}W transect on (a) 10/22/2011; (b) 11/10/2011; (c) 11/16/2011. Right: Same as left panel but from model run without wind stress: (d), (e) and (f).

Figure 01

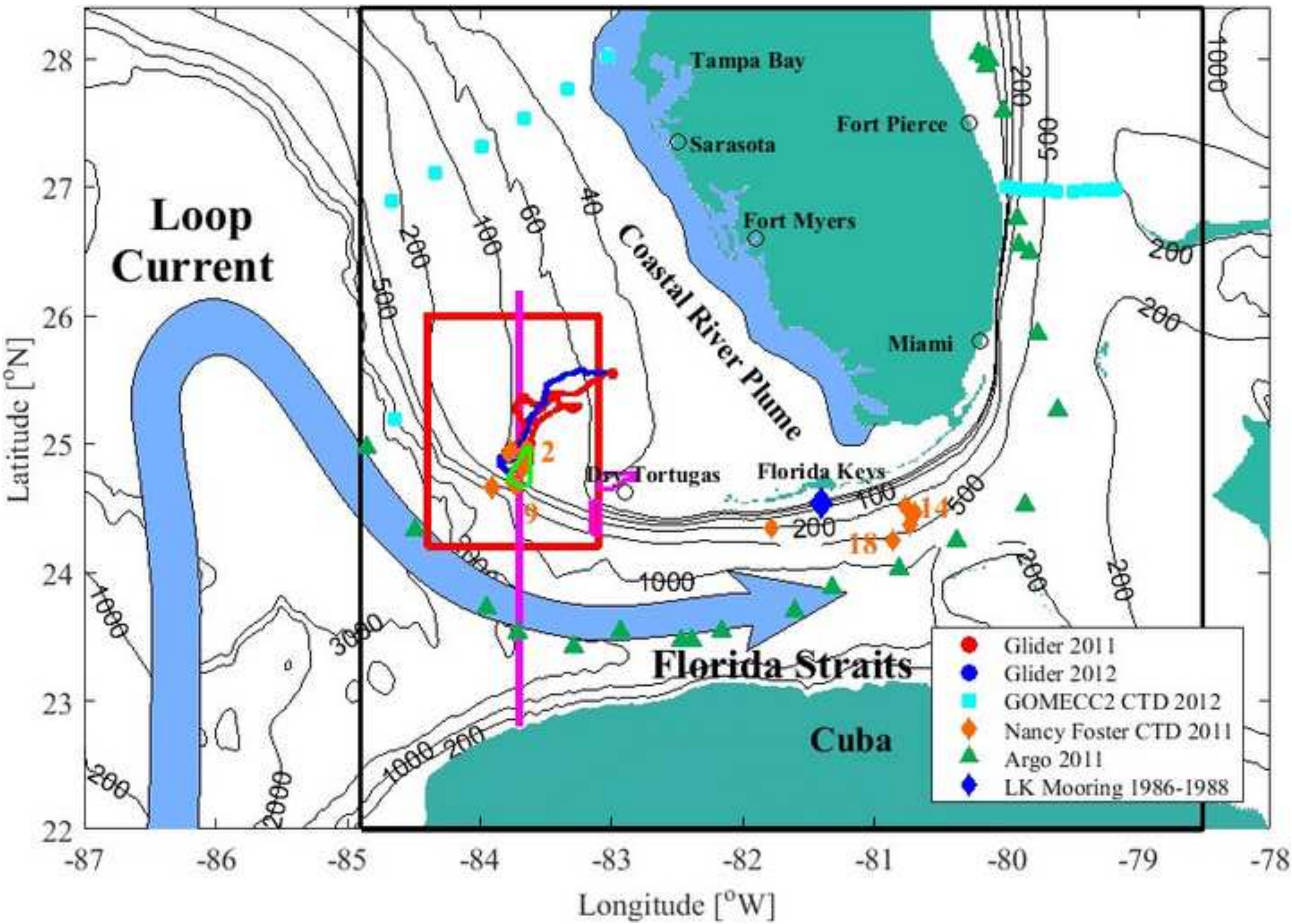

Loop Current
Coastal River Plume
Tampa Bay
Sarasota
Fort Myers
Fort Pierce
Miami
Dry Tortugas
Florida Keys
Florida Straits
Cuba
Latitude [°N]
Longitude [°W]
Glider 2011
Glider 2012
GOMECC2 CTD 2012
Nancy Foster CTD 2011
Argo 2011
LK Mooring 1986-1988

Figure 02

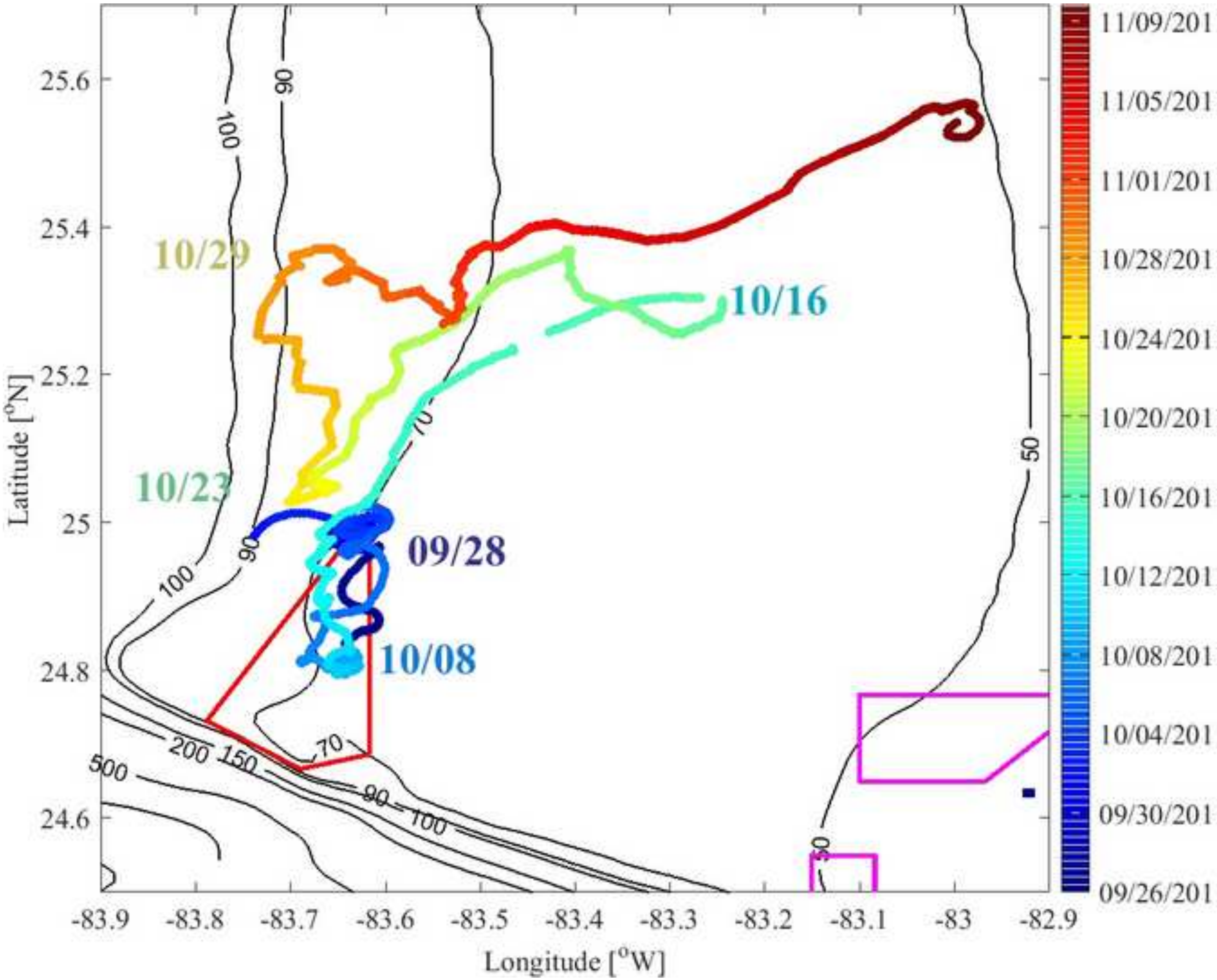

25.6
25.4
25.2
25
24.8
24.6
Latitude [^{o}N]
-83.9
-83.8
-83.7
-83.6
-83.5
-83.4
-83.3
-83.2
-83.1
-83
-82.9
Longitude [^{o}W]
10/29
10/16
10/23
09/28
10/08
90
100
70
50
200
150
500
11/09/2011
11/05/2011
11/01/2011
10/28/2011
10/24/2011
10/20/2011
10/16/2011
10/12/2011
10/08/2011
10/04/2011
09/30/2011
09/26/2011

Figure 03

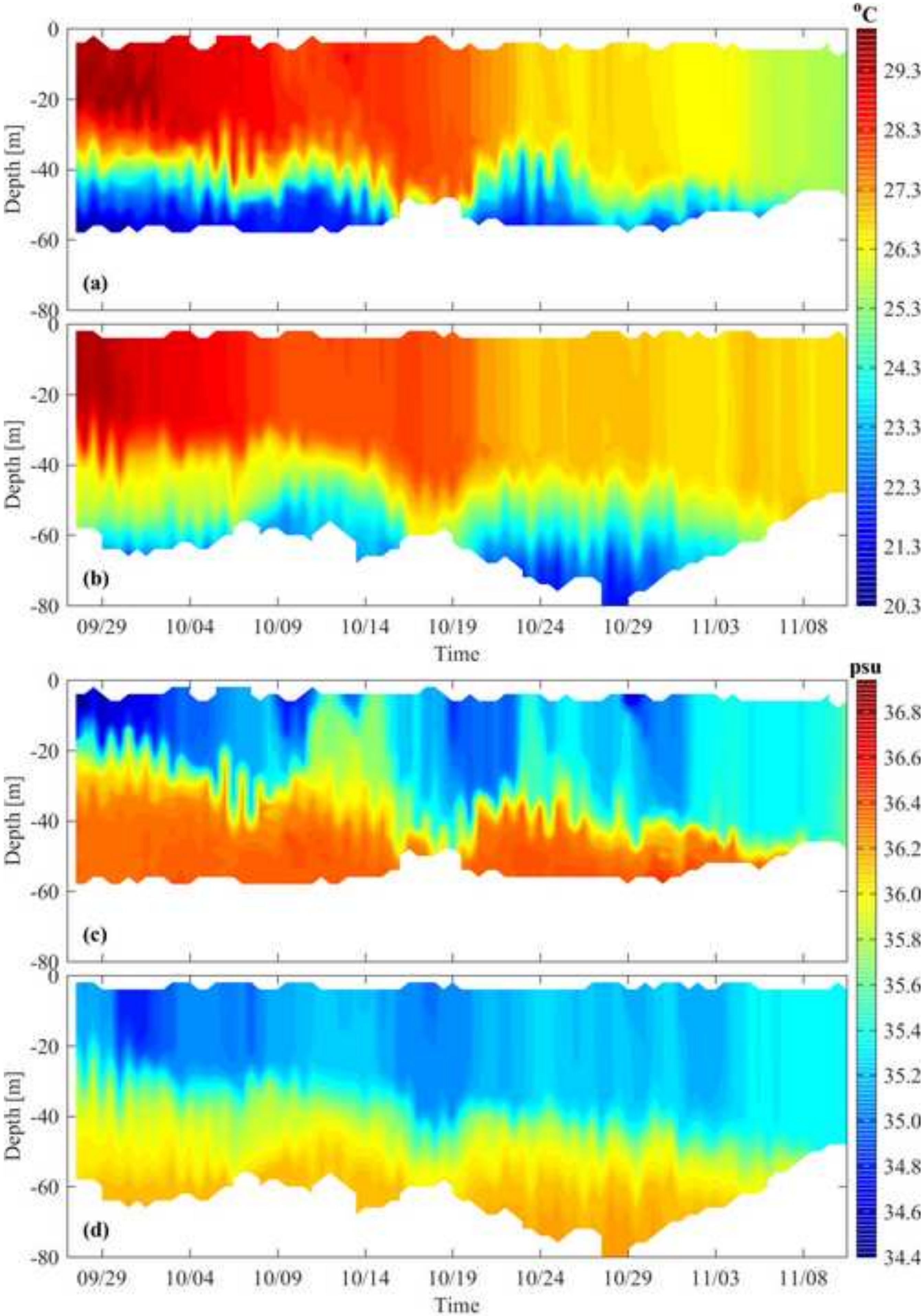

°C
psu
(a)
(b)
(c)
(d)
Depth [m]
Time
0
-20
-40
-60
-80
09/29
10/04
10/09
10/14
10/19
10/24
10/29
11/03
11/08
29.3
28.3
27.3
26.3
25.3
24.3
23.3
22.3
21.3
20.3
36.8
36.6
36.4
36.2
36.0
35.8
35.6
35.4
35.2
35.0
34.8
34.6
34.4

Figure 04

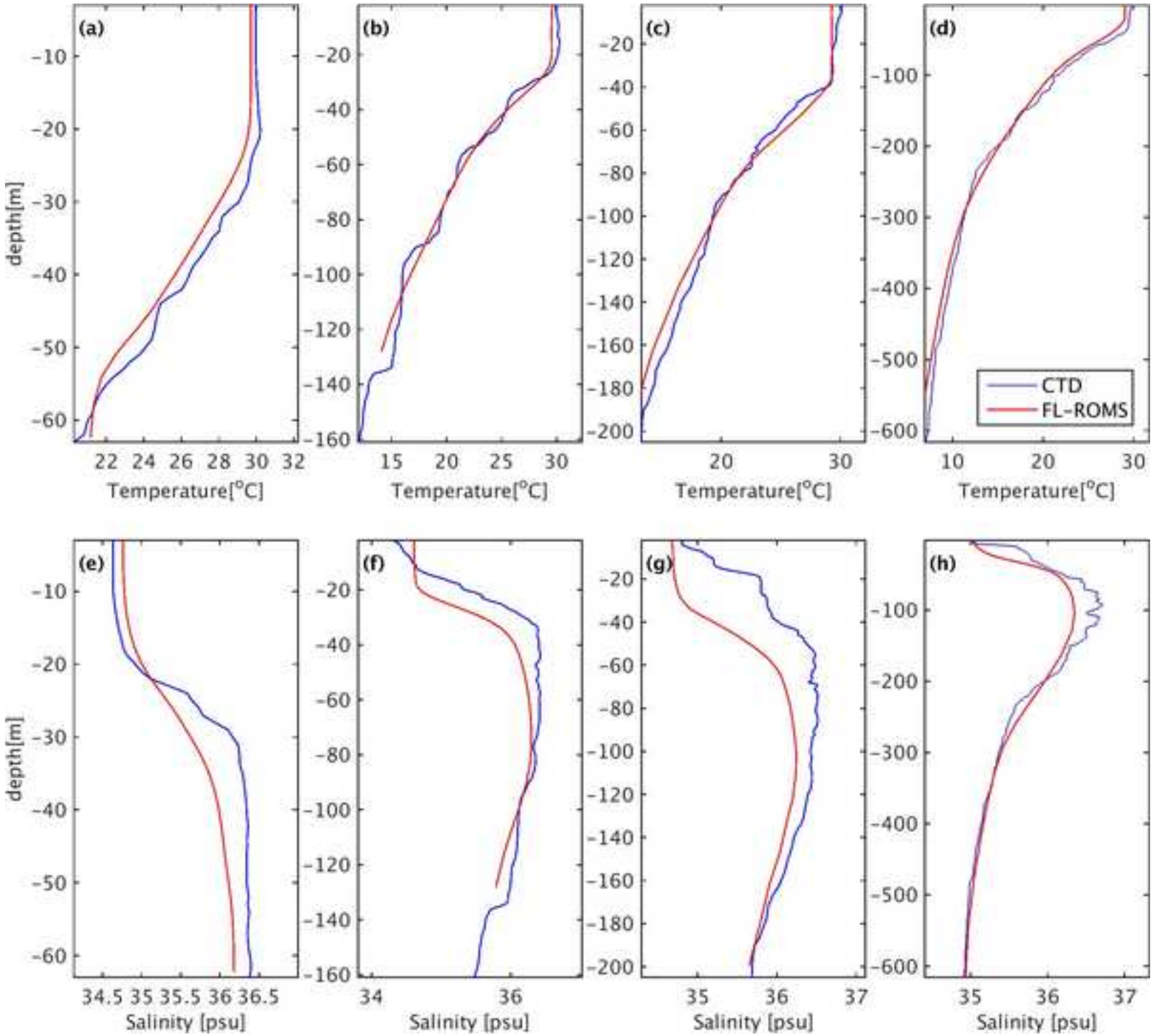

Figure 05

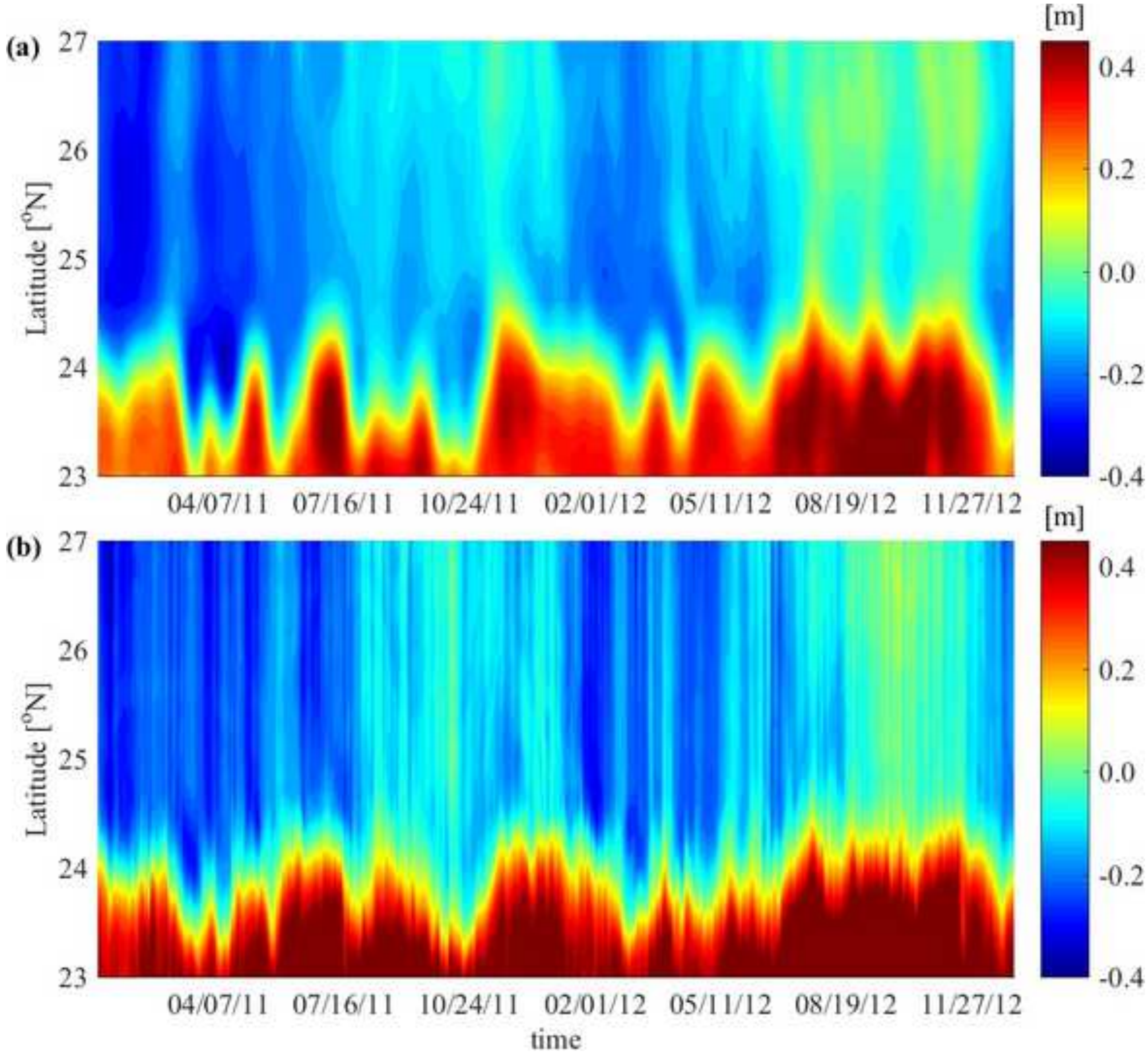

(a)
27
26
25
24
23
Latitude [°N]
04/07/11
07/16/11
10/24/11
02/01/12
05/11/12
08/19/12
11/27/12
[m]
0.4
0.2
0.0
-0.2
-0.4
(b)
27
26
25
24
23
Latitude [°N]
04/07/11
07/16/11
10/24/11
02/01/12
05/11/12
08/19/12
11/27/12
time
[m]
0.4
0.2
0.0
-0.2
-0.4

Figure 06

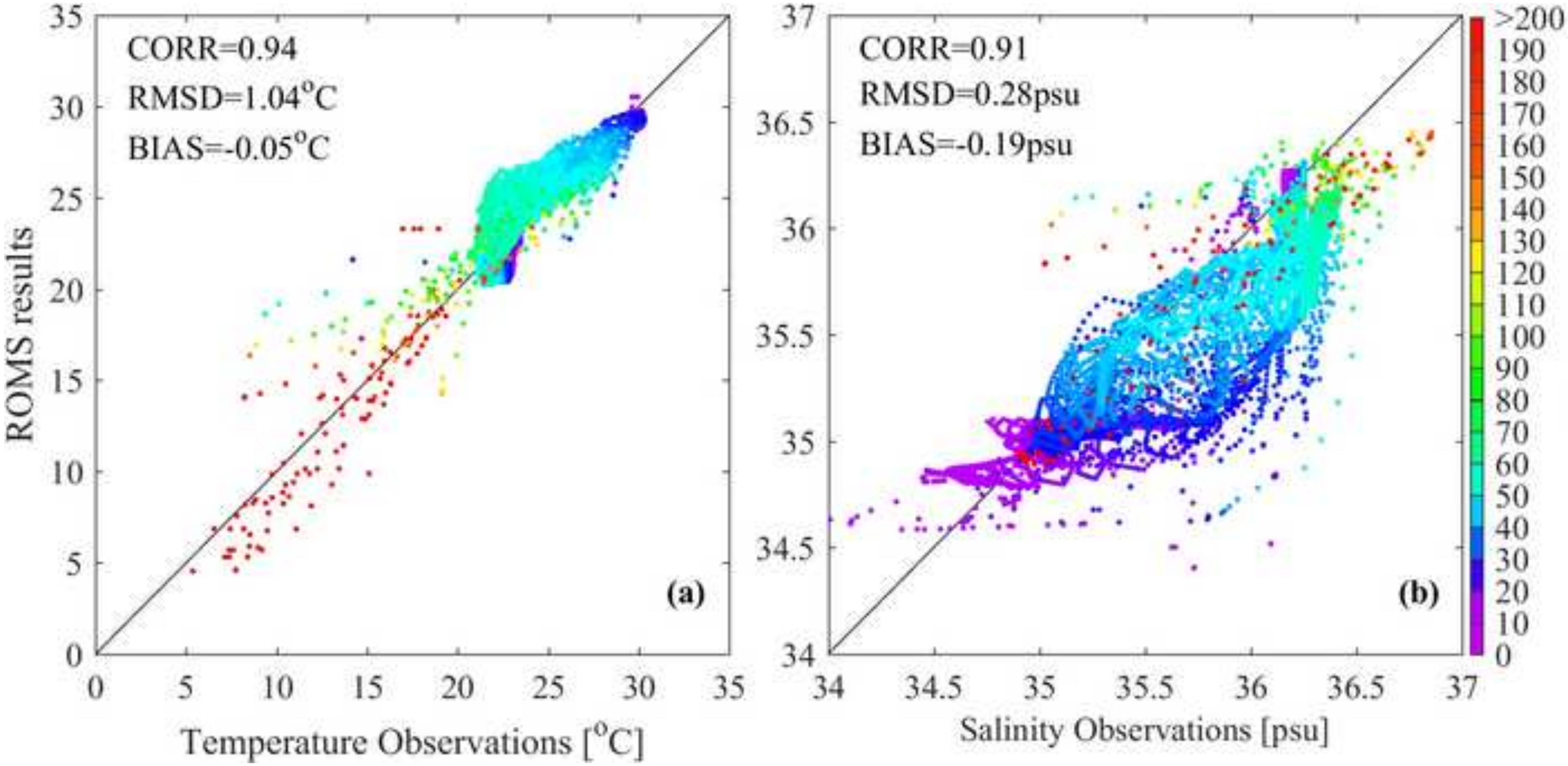
CORR=0.94
RMSD=1.04°C
BIAS=-0.05°C
(a)
ROMS results
Temperature Observations [°C]
CORR=0.91
RMSD=0.28psu
BIAS=-0.19psu
(b)
Salinity Observations [psu]
Depth [m]
>200

Figure 07

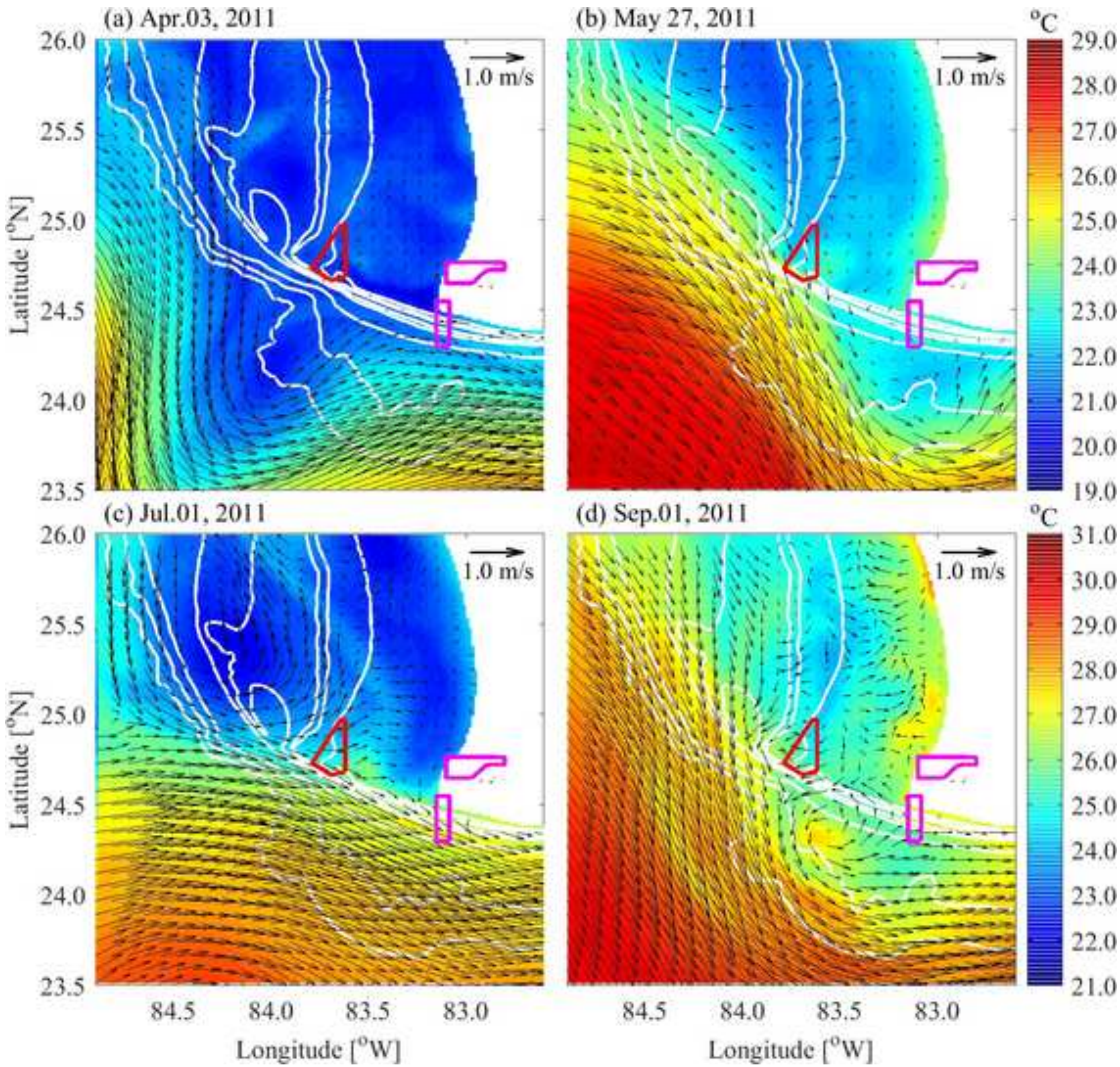

(a) Apr.03, 2011
(b) May 27, 2011
(c) Jul.01, 2011
(d) Sep.01, 2011
1.0 m/s
°C
29.0
28.0
27.0
26.0
25.0
24.0
23.0
22.0
21.0
20.0
19.0
31.0
30.0
29.0
28.0
27.0
26.0
25.0
24.0
23.0
22.0
21.0
26.0
25.5
25.0
24.5
24.0
23.5
Latitude [°N]
84.5
84.0
83.5
83.0
Longitude [°W]

Figure 08

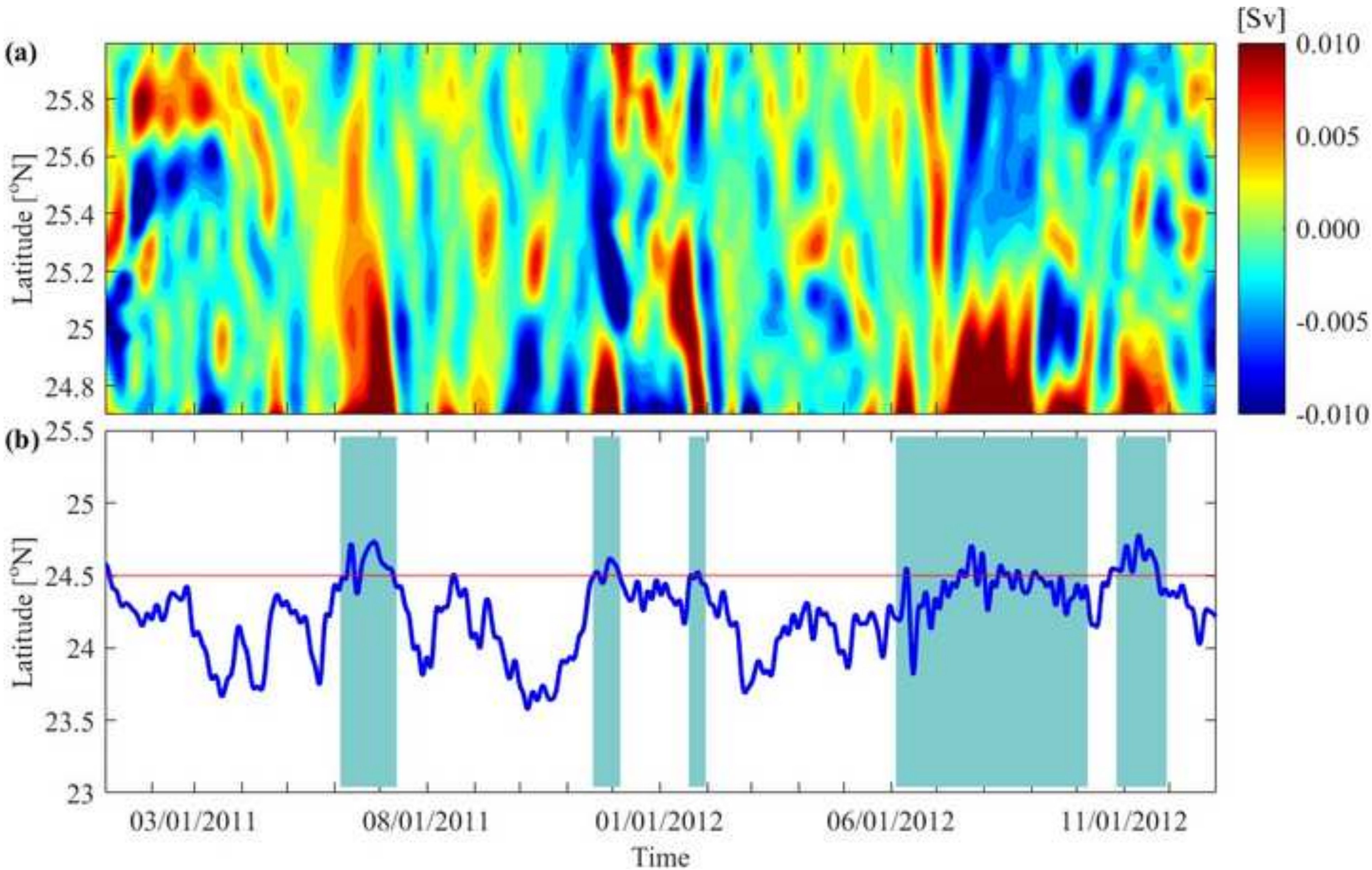

(a)
(b)
[Sv]
0.010
0.005
0.000
-0.005
-0.010
Latitude [°N]
25.8
25.6
25.4
25.2
25
24.8
25.5
24.5
24
23.5
23
03/01/2011
08/01/2011
01/01/2012
06/01/2012
11/01/2012
Time

Figure 09

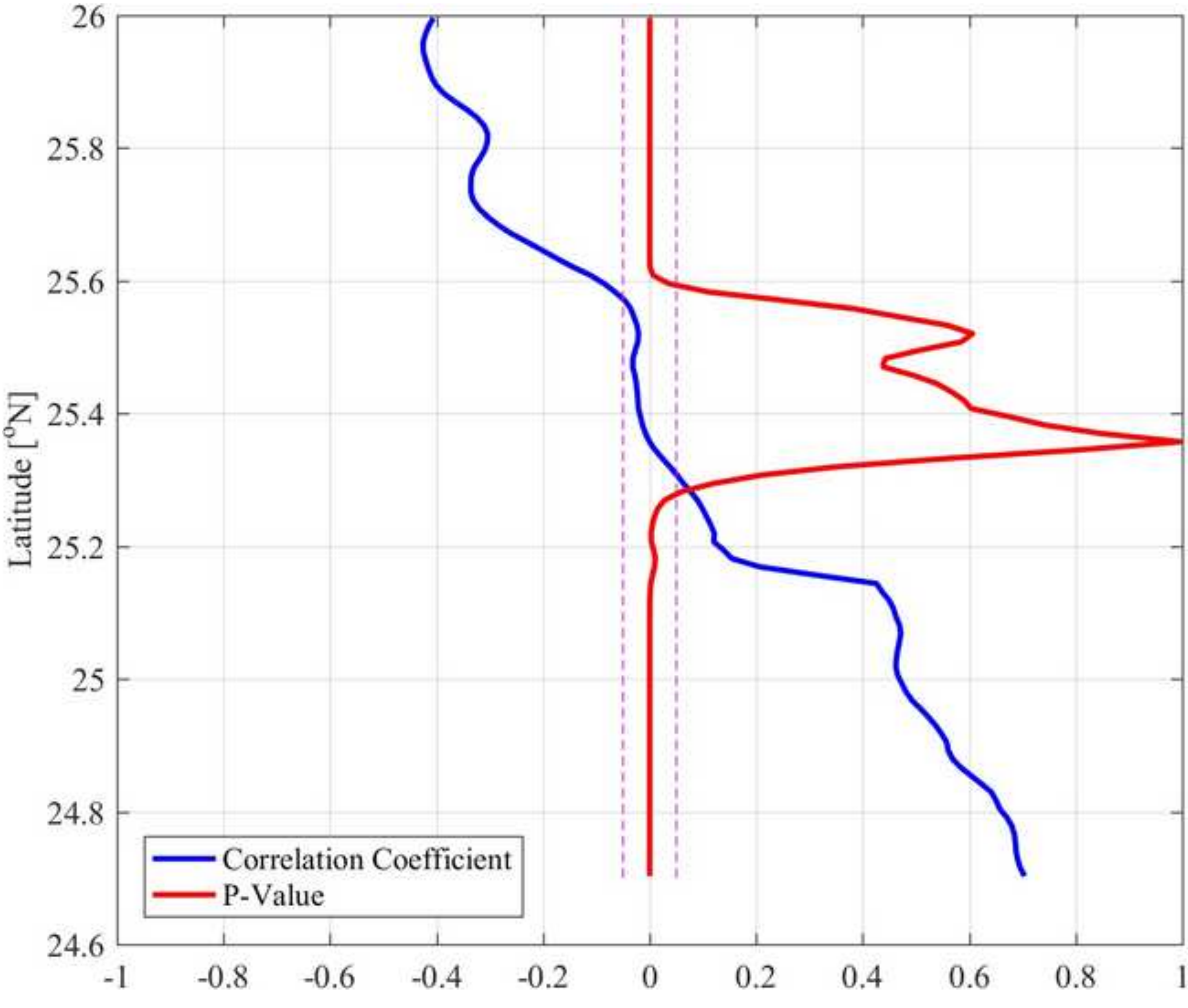
26
25.8
25.6
25.4
25.2
25
24.8
24.6
Latitude [°N]
-1
-0.8
-0.6
-0.4
-0.2
0
0.2
0.4
0.6
0.8
1
Correlation Coefficient
P-Value

Figure 10

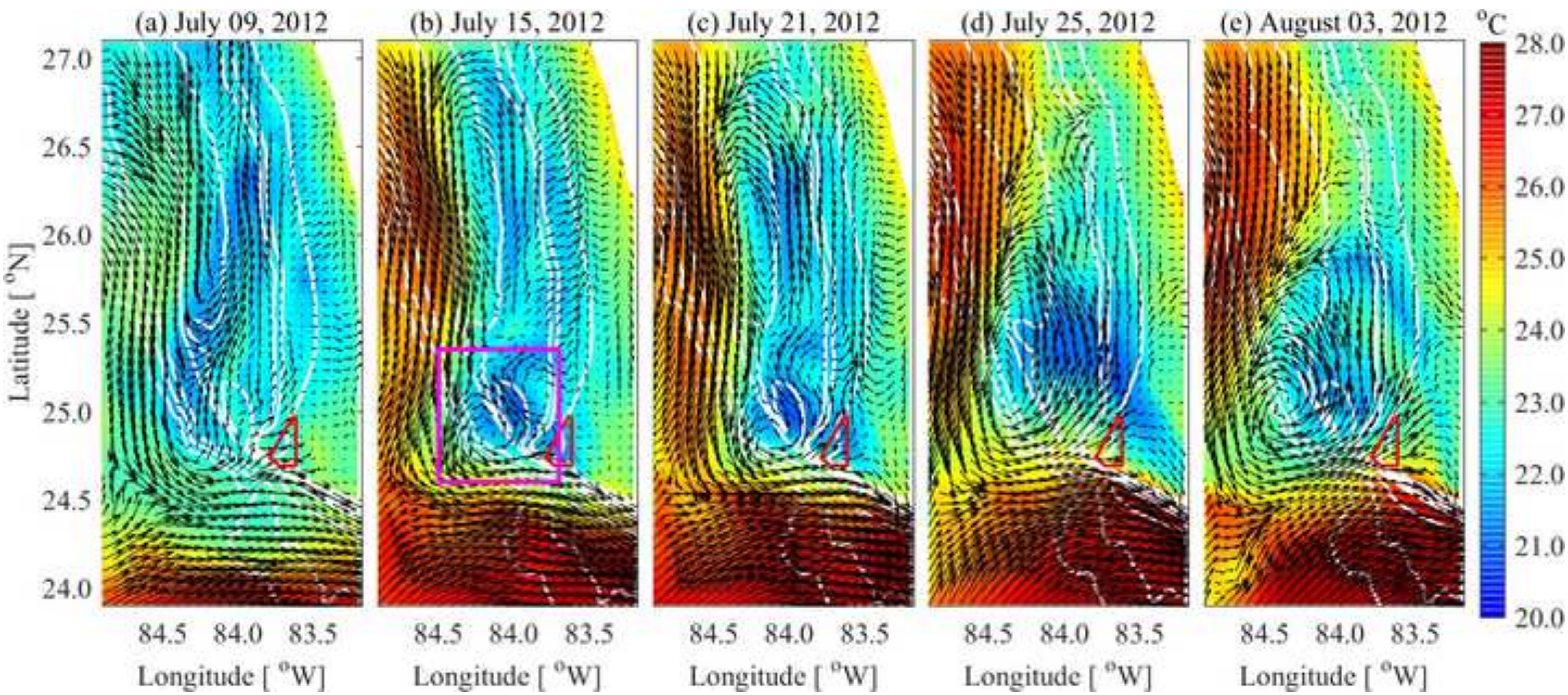
(a) July 09, 2012
(b) July 15, 2012
(c) July 21, 2012
(d) July 25, 2012
(e) August 03, 2012
°C
28.0
27.0
26.0
25.0
24.0
23.0
22.0
21.0
20.0
Latitude [°N]
27.0
26.5
26.0
25.5
25.0
24.5
24.0
84.5 84.0 83.5
Longitude [°W]

Figure 11

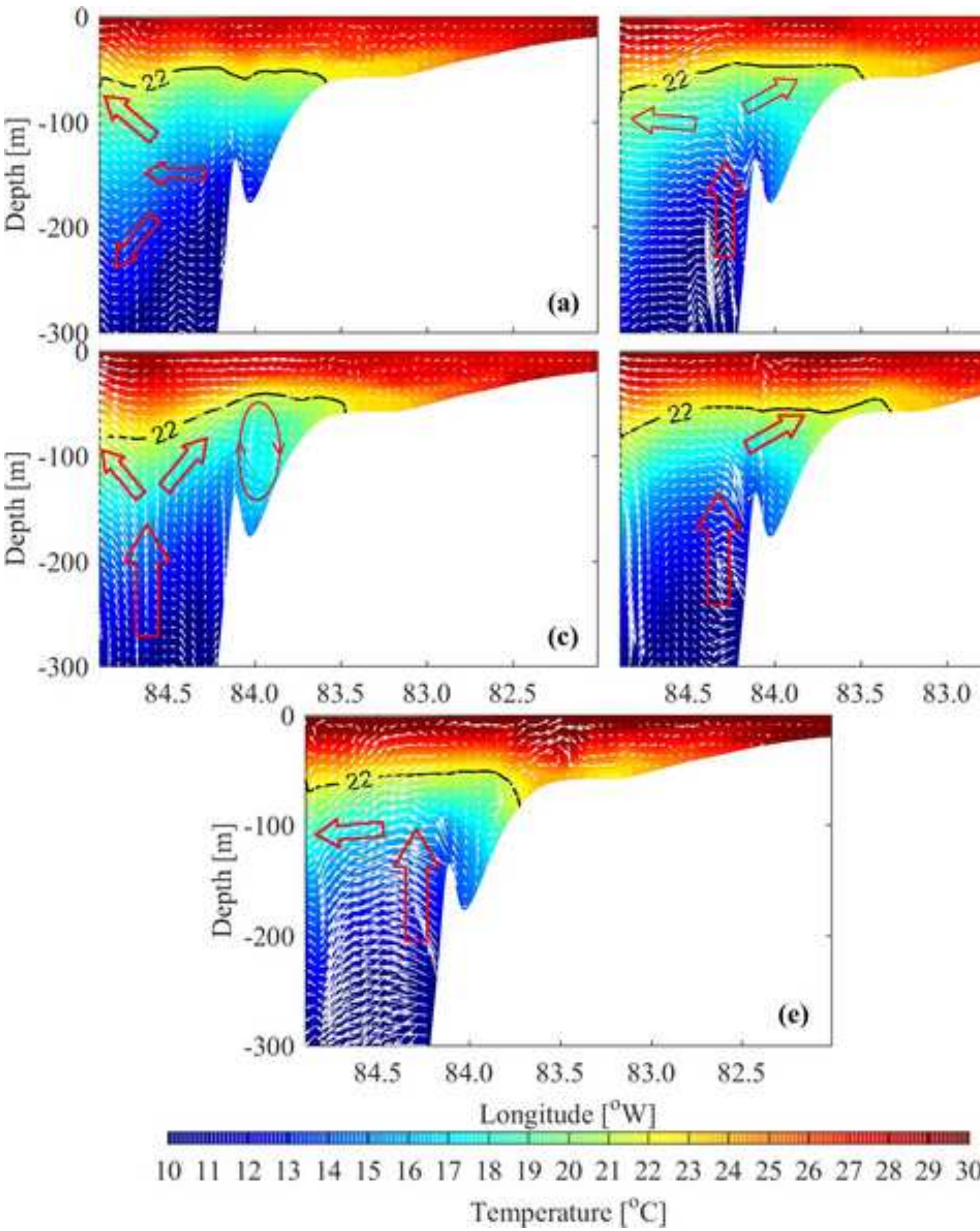

0
-100
-200
-300
Depth [m]
22
(a)
(b)
(c)
(d)
(e)
84.5
84.0
83.5
83.0
82.5
Longitude [°W]
10 11 12 13 14 15 16 17 18 19 20 21 22 23 24 25 26 27 28 29 30
Temperature [°C]

Figure 12

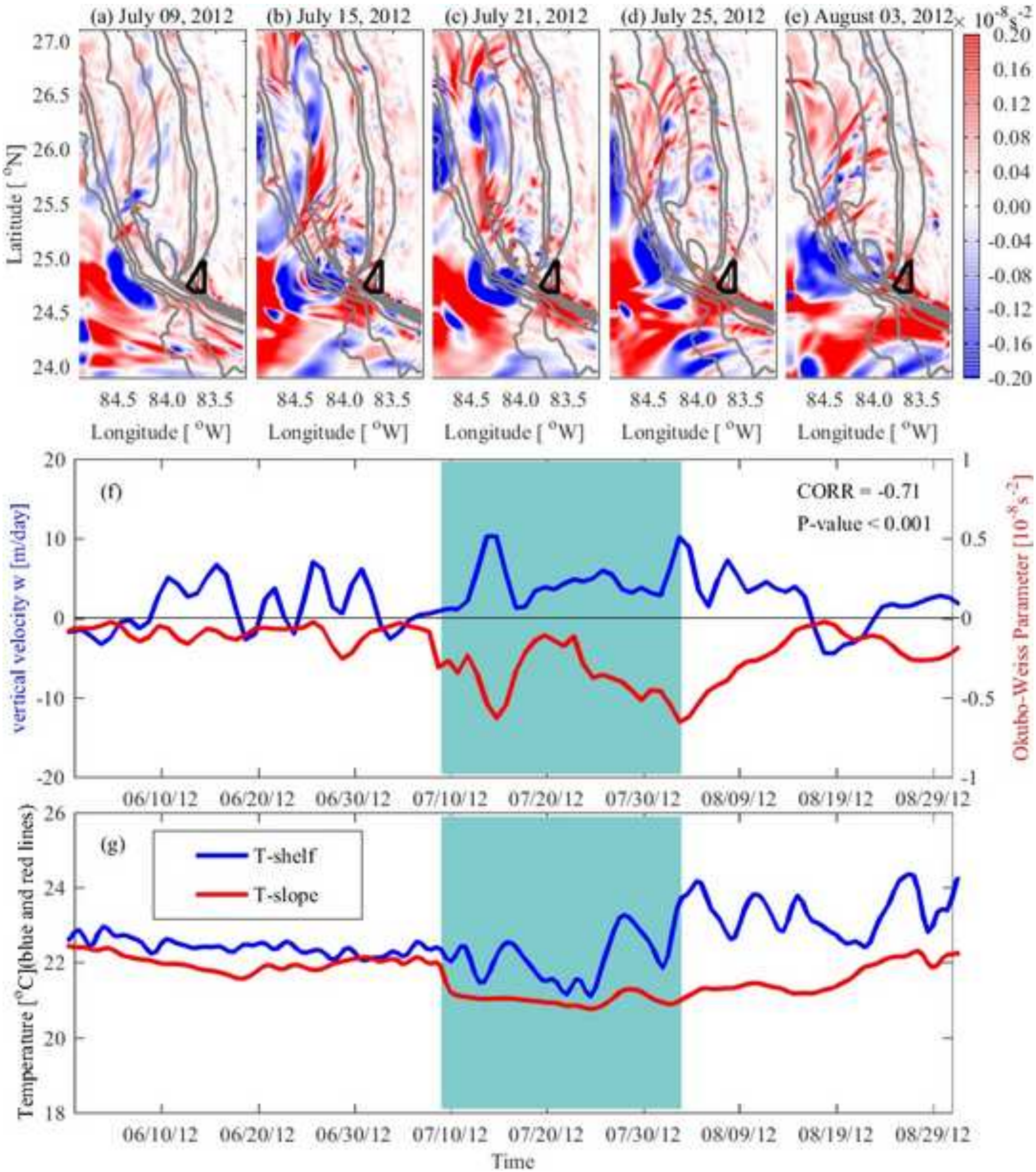

(a) July 09, 2012
(b) July 15, 2012
(c) July 21, 2012
(d) July 25, 2012
(e) August 03, 2012
× 10^{-8} s^{-2}
Latitude [°N]
Longitude [°W]
(f)
CORR = -0.71
P-value < 0.001
vertical velocity w [m/day]
Okubo-Weiss Parameter [10^{-8} s^{-2}]
(g)
T-shelf
T-slope
Temperature [°C](blue and red lines)
Time

Figure 13

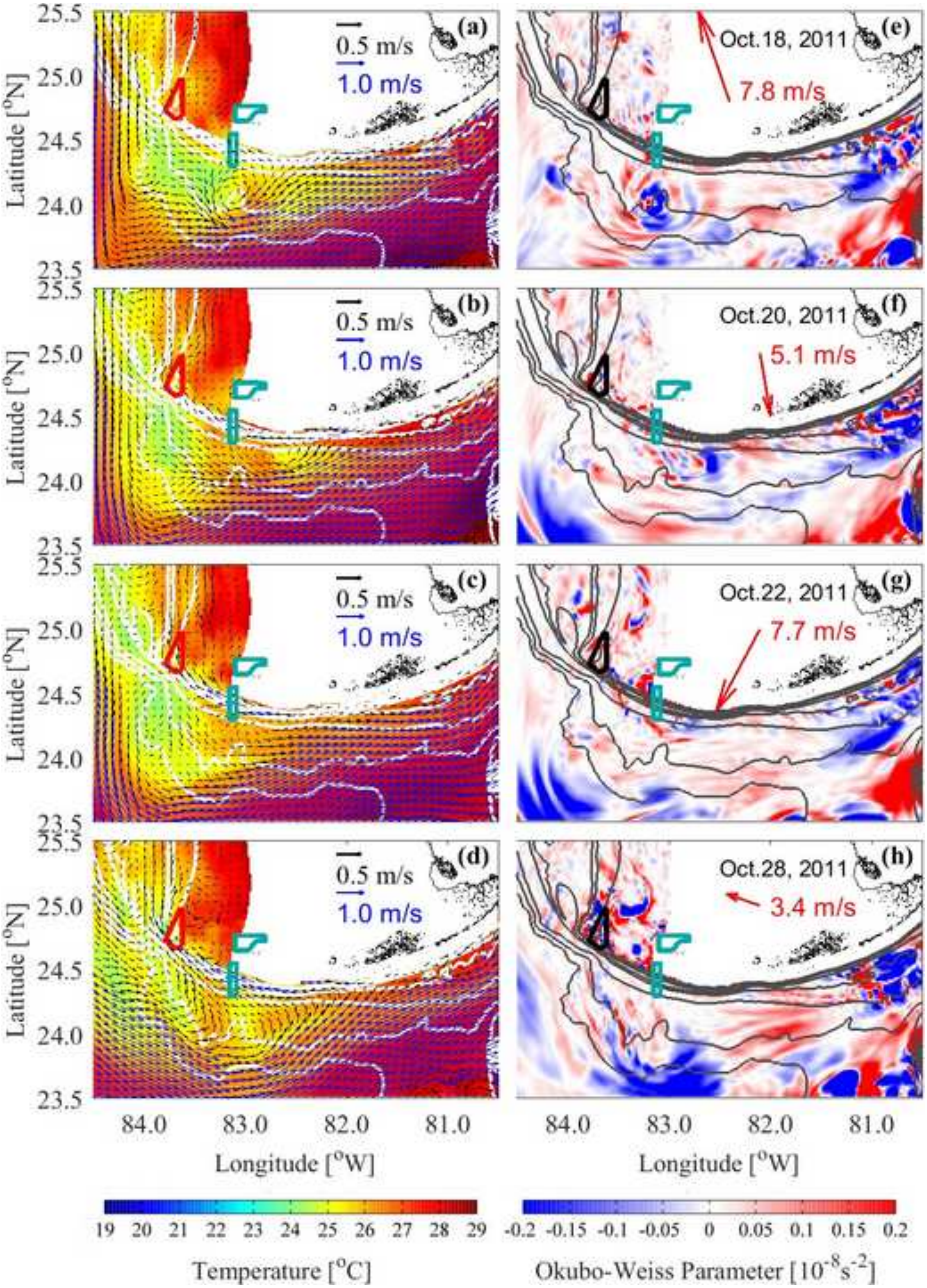
(a)
(b)
(c)
(d)
(e)
(f)
(g)
(h)
0.5 m/s
1.0 m/s
Oct.18, 2011
7.8 m/s
Oct.20, 2011
5.1 m/s
Oct.22, 2011
7.7 m/s
Oct.28, 2011
3.4 m/s
25.5
25.0
24.5
24.0
23.5
Latitude [^{o}N]
84.0
83.0
82.0
81.0
Longitude [^{o}W]
19 20 21 22 23 24 25 26 27 28 29
Temperature [^{o}C]
-0.2 -0.15 -0.1 -0.05 0 0.05 0.1 0.15 0.2
Okubo-Weiss Parameter [$10^{-8}s^{-2}$]

Figure 14

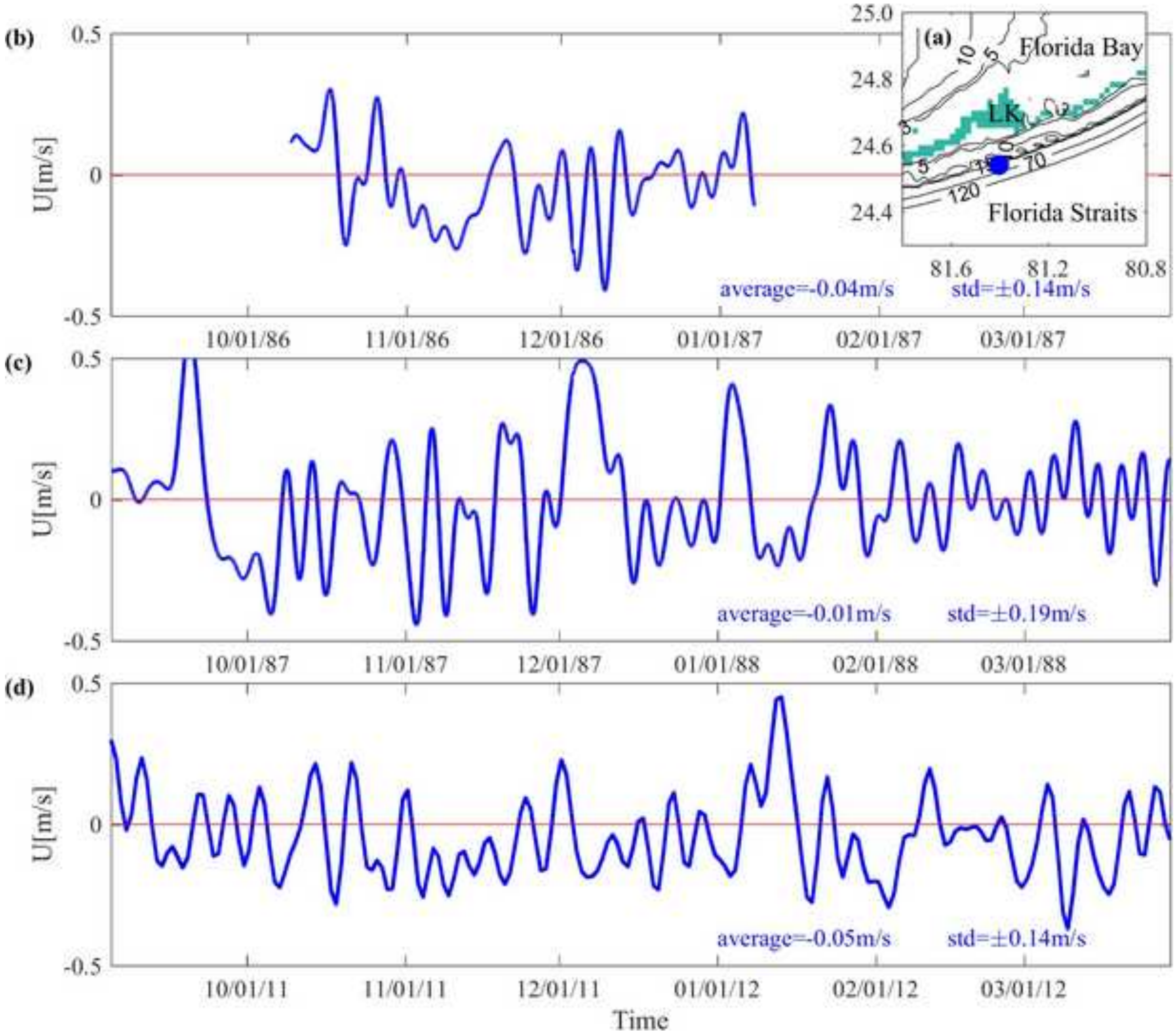

(b)
0.5
0
-0.5
U[m/s]
average=-0.04m/s
std=±0.14m/s
10/01/86
11/01/86
12/01/86
01/01/87
02/01/87
03/01/87
(a)
25.0
24.8
24.6
24.4
81.6
81.2
80.8
Florida Bay
LK
Florida Straits
10
5
70
120
(c)
0.5
0
-0.5
U[m/s]
average=-0.01m/s
std=±0.19m/s
10/01/87
11/01/87
12/01/87
01/01/88
02/01/88
03/01/88
(d)
0.5
0
-0.5
U[m/s]
average=-0.05m/s
std=±0.14m/s
10/01/11
11/01/11
12/01/11
01/01/12
02/01/12
03/01/12
Time

Figure 15

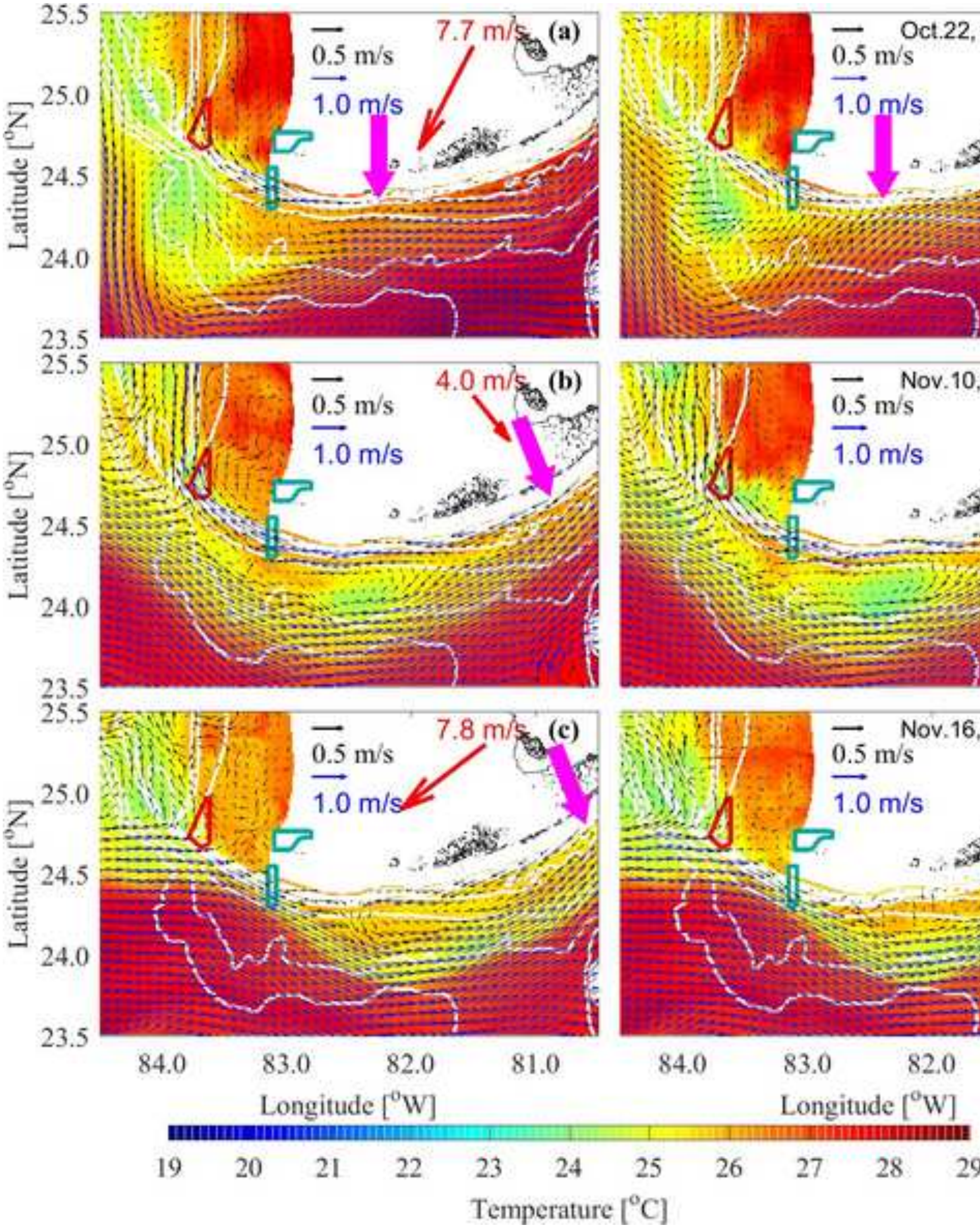

(a)
(b)
(c)
(d)
(e)
(f)
7.7 m/s
4.0 m/s
7.8 m/s
Oct.22, 2011
Nov.10, 2011
Nov.16, 2011
0.5 m/s
1.0 m/s
Latitude [°N]
Longitude [°W]
Temperature [°C]
25.5
25.0
24.5
24.0
23.5
84.0
83.0
82.0
81.0
19
20
21
22
23
24
25
26
27
28
29

Figure 16

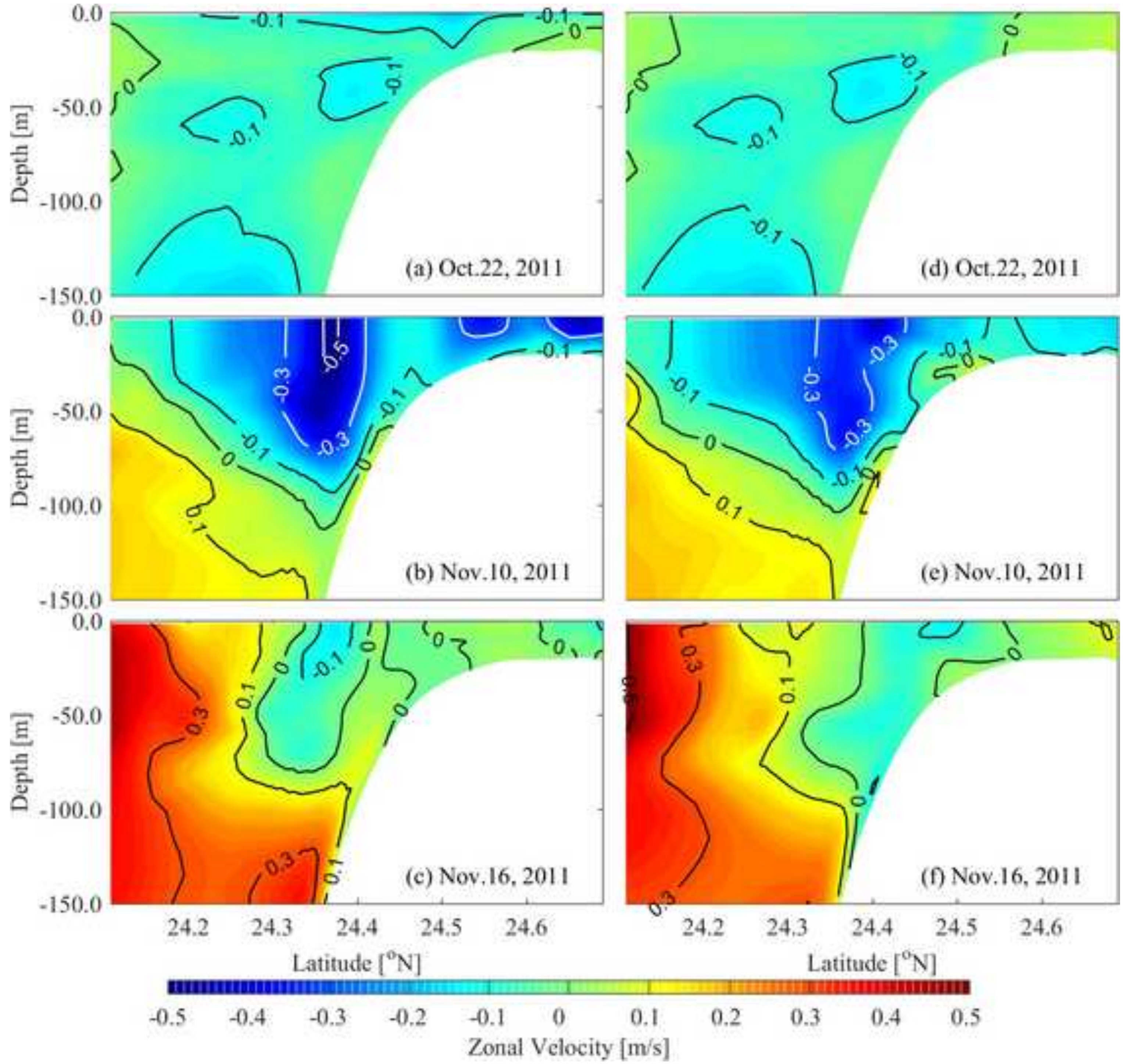

(a) Oct.22, 2011
(b) Nov.10, 2011
(c) Nov.16, 2011
(d) Oct.22, 2011
(e) Nov.10, 2011
(f) Nov.16, 2011
Depth [m]
Latitude [°N]
Zonal Velocity [m/s]